Title

Environmental cystine drives glutamine anaplerosis and sensitizes cells to glutaminase inhibition

Running Title

Cystine promotes glutamine anaplerosis

Authors

Alexander Muir[1], Laura V. Danai[1], Dan Y. Gui[1], Chiara Y. Waingarten[1] and Matthew G. Vander Heiden[1,2#]

[1] Koch Institute for Integrative Cancer Research and Department of Biology, Massachusetts Institute of Technology, Cambridge, MA 02139, USA
[2] Dana-Farber Cancer Institute, Boston, MA 02115, USA
[#] Correspondence: mvh@mit.edu

Abstract

Many cancer cell lines depend on extracellular glutamine as a major tri-carboxylic acid (TCA) cycle anaplerotic substrate to support proliferation *in vitro*. However, recent studies have suggested that some cells that depend on glutamine anaplerosis in culture rely much less on glutamine catabolism to proliferate *in vivo*, with environmental differences between tumors and cell culture influencing the extent of glutamine catabolism. Here we sought to better understand the environmental differences that cause differential dependence on glutamine for TCA cycle anaplerosis. We find that cells cultured in adult bovine serum, a condition that more closely reflects the nutrients available to cells *in vivo*, leads to decreased glutamine catabolism and reliance on glutamine anaplerosis compared to standard tissue culture conditions. By analyzing the nutrient differences between bovine serum and media, we find that levels of a single nutrient, cystine, can account for the differential dependence on glutamine in these different environmental contexts. Further, we show that cystine levels dictate glutamine dependence via the cystine/glutamate antiporter xCT/*SLC7A11*, and that environmental cystine levels in conjunction with xCT/*SLC7A11* expression is necessary and sufficient to drive increased

glutamine anaplerosis, defining important determinants of glutamine anaplerosis and glutaminase dependence in cancer cells.

Introduction

Altered metabolism is a hallmark of cancer (Hanahan and Weinberg, 2011) and reflects the increased energetic and biosynthetic demands of proliferating cancer cells (DeBerardinis and Chandel, 2016; Vander Heiden and DeBerardinis, 2017). Indeed, one of the earliest noted biochemical differences between cancerous and normal tissues is increased uptake of glucose and glycolysis in tumors (Cori and Cori, 1925; Warburg et al., 1927). Beyond increased glucose metabolism in tumors, another long standing observation is that many cancer cells consume substantial amounts of glutamine in culture, far in excess of other amino acids (Eagle, 1955; Jain et al., 2012). Consistent with this, many cancer cell lines depend on extracellular glutamine for proliferation *in vitro*, even though glutamine is nominally non-essential and can be synthesized from other nutrients. This contributed to the concept that some cancer cells are glutamine addicted (Altman et al., 2016; Wise and Thompson, 2010).

Glutamine can be used to support proliferation in multiple ways. It is a proteinogenic amino acid, can act as a nitrogen donor for the synthesis of amino acids as well as nucleotides, and glutamine can contribute carbon to the TCA cycle to replace cycle intermediates that are removed for the production of biomass, a process termed anaplerosis (Altman et al., 2016; Daye and Wellen, 2012; DeBerardinis and Cheng, 2010; Hensley et al., 2013). Analysis of the fate of glutamine nitrogen in proliferating cancer cells *in vitro* suggests that most glutamine nitrogen is excreted as ammonia and alanine, suggesting that the high rate of glutamine consumption is not due to nitrogen demand (DeBerardinis et al., 2007). Instead, glutamine metabolism is important for TCA cycle anaplerosis in multiple contexts (Altman et al., 2016; DeBerardinis et al., 2007; Yuneva et al., 2007). Across multiple cancer cell lines, the majority of aspartate, glutamate and TCA cycle metabolites are glutamine-derived (Altman et al., 2016;

Wise and Thompson, 2010), with production of amino acids being a major fate of anaplerotic glutamine carbon (Hosios et al., 2016). In line with these results, proliferation of many cell types under glutamine starvation is rescued by providing an alternative source of the TCA cycle intermediates α-ketoglutarate (αKG) (van den Heuvel et al., 2012; Wise et al., 2008; Wise et al., 2011) or oxaloacetate (Patel et al., 2016). Collectively, these results suggest that anaplerosis contributes to the large cellular consumption of glutamine in culture, and to dependence on this amino acid for cell proliferation and survival.

Glutamine can enter the TCA cycle through multiple metabolic routes. First, several transporters are capable of transporting glutamine into cells (Hediger et al., 2013; Hyde et al., 2003). Relevant to cancer, the neutral amino acid transporters ASCT2/*SLC1A5* and LAT1/*SLC7A5* are known to have higher expression in certain tumors, and can mediate glutamine uptake in cell lines derived from these tumors (Bhutia et al., 2015; Pochini et al., 2014). Intracellularly, glutamine is converted to glutamate either by donating the amide nitrogen for the production of nucleotides or asparagine, or by glutaminase activity (encoded by *GLS1 or GLS2*), which produces glutamate and ammonia from glutamine (Curthoys and Watford, 1995; Krebs, 1935). In proliferating cells, glutaminase activity can be the primary driver of glutamate production from glutamine, as amide nitrogen incorporation into mass is low compared to release of glutamine nitrogen as ammonia (Brand, 1985; Brand et al., 1986; Hosios et al., 2016; Wise et al., 2008). Genetic or pharmacological loss of *GLS1* activity depletes TCA metabolites and slows proliferation of a variety of cancer cell lines in culture (Cheng et al., 2011; Gameiro et al., 2013; Gao et al., 2009; Gross et al., 2014; Le et al., 2012; Seltzer et al., 2010; Son et al., 2013; Timmerman et al., 2013; van den Heuvel et al., 2012; Wang et al., 2010; Yuneva et al., 2012). This has led to interest in targeting glutaminase activity therapeutically, and the glutaminase inhibitor CB-839 is being evaluated in clinical trials for cancer therapy (Gross et al., 2014). In the last step of glutamine carbon entry into the TCA cycle, glutamate produced from glutamine is converted to αKG by either transamination reactions or by glutamate

dehydrogenase to produce αKG as an anaplerotic TCA cycle intermediate (Moreadith and Lehninger, 1984). Rapidly proliferating cells have been shown to preferentially use transamination reactions for αKG production, consistent with their increased need for nitrogen for biosynthetic demand (Coloff et al., 2016). Finally, consistent with these observations of increased glutamine catabolism and dependence in rapidly proliferating cultured cells, glutamine catabolic pathways are controlled by oncogene expression and upregulated in many cancer cell lines (Altman et al., 2016).

Tumor cell environment can also influence dependence on glutaminase for anaplerosis and proliferation. Tracing of glucose and glutamine fate in tumors derived from human non-small cell lung cancer (NSCLC) and mouse *KRAS*-driven NSCLC found that these tumors rely more on glucose than on glutamine for TCA cycle anaplerosis (Davidson et al., 2016; Hensley et al., 2016; Sellers et al., 2015). This correlated with resistance of these tumors to glutaminase inhibition *in vivo*; but surprisingly, cell lines derived from these tumors with decreased glutamine catabolism showed dramatically increased glutamine anaplerosis and sensitivity to glutaminase inhibition when cultured *in vitro* (Davidson et al., 2016). These results suggest that, even for cells capable of glutamine catabolism, environmental differences between tumors *in vivo* and tissue culture dictates the use of glutamine for anaplerosis.

We describe the identification of an environmental factor that contributes to differential glutamine anaplerosis between human NSCLC tumors growing *in vivo* and cell lines cultured *in vitro*. Nutrient availability is different for cancer cells growing as tumors *in vivo* compared to culture conditions *in vitro*, and we explored the role of nutrient environment by culturing the human A549 NSCLC cell line in adult bovine serum, a medium that more closely models *in vivo* nutrient levels. In this condition, the contribution of glutamine carbon to the TCA cycle decreases to levels observed for A549 tumors growing *in vivo*. Culture in adult bovine serum also induces glutaminase inhibitor resistance, a phenotype seen for NSCLC tumors *in vivo*. Deconvolution of differences in media composition showed that levels of a single nutrient,

cystine (the oxidized dimer of the amino acid cysteine), largely dictates the observed differences in glutamine anaplerosis and dependence. Further, we find that cystine regulation of glutamine anaplerosis depends on expression of the cystine/glutamate antiporter xCT (encoded by the gene *SLC7A11*). Lastly, we find that administration of cystine to tumor bearing mice increases tumor glutamine anaplerosis *in vivo*. Collectively, these results suggest that environmental cystine availability and xCT/*SLC7A11* expression are critical determinants of glutamine anaplerosis and glutaminase dependence. They also highlight how nutrient conditions can impact cell metabolism.

Results

Cells in vivo *or cultured in adult bovine serum exhibit limited glutamine catabolism compared to cells cultured in standard tissue culture conditions*

Mutant *Kras*-driven mouse lung cancer cells exhibit differences in glutamine metabolism dictated by their environment, such that glutamine extensively labels TCA cycle intermediates in cell culture but not in tumors (Davidson et al., 2016). To confirm this finding, we examined glutamine metabolism in mutant *KRAS*-driven human A549 lung cancer cells cultured in multiple environments. For these studies, we used gas chromatography-mass spectrometry (GC-MS) to trace the fate of glutamine where all five carbons are ^{13}C labeled ([U-$^{13}C_5$]glutamine) in each environment, focusing on whether glutamine carbon contributed to the TCA cycle (Figure 1A). First, we verified that glutamine was not a major source of TCA cycle carbon in subcutaneous A549 xenograft tumors. For these studies [U-$^{13}C_5$]glutamine was infused into tumor bearing animals for 6h to achieve a final enrichment of ~35% labeled glutamine in plasma and ~25% in tumors (Fig. 1B). Consistent with previous results (Davidson et al., 2016), upon [U-$^{13}C_5$]glutamine infusion, there was less labeling of glutamate, TCA cycle intermediates and aspartate in the tumors despite the presence of labeled glutamine (Fig. 1B). These findings suggest that glutamine is not a major source of TCA cycle carbon in A549-derived tumors *in*

vivo. Normalization of tumor m+5 glutamate label to m+5 glutamine labeling indicates that only ~25% of glutamate is derived from glutamine in these tumors. In contrast, when A549 cells are cultured in RPMI-based media with [U-$^{13}C_5$]glutamine added to a similar enrichment of ~33%, we find that ~27% of glutamate is glutamine derived, which when normalized to glutamine enrichment indicates that 80% of glutamate is derived from glutamine under these conditions (Fig. 1C). Additionally, when the cells are cultured in RPMI, more than 60% of the carbon in aspartate and other TCA cycle intermediates was derived from glutamine (Fig. 1C). This is consistent with glutamine being a major TCA cycle carbon source for A549 cells in culture, and demonstrates that compared to standard culture conditions tumors derived from these cells use less glutamine *in vivo*.

To begin to examine the environmental factors that contribute to this difference in glutamine metabolism, we cultured cells in adult bovine serum based on the notion that this may better reflect the nutrient levels available from the circulation to the cells in tumors. For these studies, we added [U-$^{13}C_5$]glutamine to adult bovine serum to achieve an enrichment of ~33% that is comparable to the labeled glutamine enrichment observed in plasma and tumors *in vivo*. We then traced the fate of ^{13}C carbon into the TCA cycle and found substantially less labeling of glutamate, aspartate and TCA cycle metabolites compared to cells cultured in RPMI-based media (Fig. 1C). In fact, only ~35% of glutamate was estimated to be derived from glutamine when cells were cultured in adult bovine serum. We verified that glutamine labeling reached isotopic steady state after 8 hours of culture in adult bovine serum (Figure 1 Supplement 1), suggesting that these labeling differences were not explained by differences in labeling kinetics. Importantly, the decrease in glutamine-derived label observed in A549 cells cultured in adult bovine serum was not specific to bovine serum or to serum products, as the contribution of glutamine carbon to glutamate and TCA cycle intermediates was similarly reduced in adult bovine heparinized plasma and adult human serum (Figure 1 Supplement 2). Thus, culturing

A549 cells in serum or plasma results in reduced glutamine catabolism to support TCA cycle anaplerosis, mimicking the results observed for A549 tumors *in vivo*.

Sensitivity of *Kras*-driven mouse lung cancer cells to the glutaminase inhibitor CB-839 correlates with glutamine carbon contribution to the TCA cycle, such that tumors derived from these cells *in vivo* were insensitive to CB-839 while proliferation of the same cells is inhibited *in vitro* (Davidson et al., 2016). Consistent with these findings, we find that A549 cells cultured in RPMI are also sensitive to CB-839, but the same cells become resistant to CB-839 when cultured in adult bovine serum (Fig. 1D). Thus, A549 cells cultured in bovine serum exhibit decreased glutamine metabolism and become resistant to glutaminase inhibitors, adopting a metabolic phenotype with regards to glutamine metabolism that is more similar to lung tumors *in vivo* than to lung cancer cells cultured in standard tissue culture media.

Differences in the small molecule fraction between RPMI and adult bovine serum affect glutamine use for TCA cycle anaplerosis

We next sought to identify factors that are different between RPMI and adult bovine serum that account for the observed differences in glutamine anaplerosis and dependence. Dialysis experiments were used to determine whether differences in the small molecule (<3.5 kDa) or large molecule (>3.5 kDa) fractions accounted for differences in glutamine contribution to the TCA cycle. First, we dialyzed a small volume of RPMI against large volumes of adult bovine serum using 3.5 kDa cutoff dialysis cassettes (Fig. 2A). This medium termed ‘adult bovine serum → RPMI,’ contained the small molecule fraction from adult bovine serum and the large molecule fraction from RPMI-based media. Similarly, we dialyzed adult bovine serum against RPMI to generate ‘RPMI → adult bovine serum,’ containing RPMI small molecules and the adult bovine serum large molecule fraction (Fig. 2A). Cells could be cultured in both media conditions, allowing us to trace the fate of [U-$^{13}C_5$]glutamine in A549 cells cultured in each media. Similar to cells grown in adult bovine serum, cells grown in ‘adult bovine serum → RPMI’

exhibited low fractional labeling of glutamate, aspartate and TCA cycle metabolites (Fig. 2B). In contrast, cells grown in 'RPMI → adult bovine serum' exhibited higher labeling of aspartate and TCA cycle intermediates from glutamine, similar to cells grown in RPMI (Fig. 2B). These differences in glutamine contribution to the TCA cycle also correlated with the ability of CB-839 to inhibit proliferation, as A549 cell proliferation is inhibited by CB-839 when cells are cultured in 'RPMI → adult bovine serum' but is largely unaffected when cultured in 'adult bovine serum → RPMI' (Fig. 2C). Similar dialysis experiments were performed with DMEM and adult bovine serum. Consistent with the RPMI dialysis experiments, 'adult bovine serum → DMEM' cultured cells displayed levels of glutamine anaplerosis and CB-839 sensitivity that were similar to cells cultured in adult bovine serum, while 'DMEM → adult bovine serum' had increased CB-839 sensitivity, similar to cells cultured in DMEM (Figure 2 Supplement 1). Taken together, these experiments suggest that differences in the small molecule fraction of standard tissue culture media and adult bovine serum largely explain the differences in glutamine anaplerosis and glutaminase inhibitor sensitivity.

Environmental cystine availability increases glutamine anaplerosis

We next considered differences in the small molecule fraction of adult bovine serum and RPMI/DMEM that could give rise to the differences in glutamine anaplerosis and CB-839 sensitivity. RPMI and DMEM both contain excess glucose, amino acids and micronutrients compared to blood (Mayers and Vander Heiden, 2015). In fact, DMEM formulations designed to have more physiological concentrations of glucose and amino acids nutrients were previously reported to alter central carbon metabolism and glutamine dependence (Schug et al., 2015; Tardito et al., 2015). In order to determine if excess nutrients in standard media formulations potentiate glutamine anaplerosis and dependence, we determined the concentration of amino acids, glucose, and pyruvate in the sera used to culture cells in this study (Table 1). We supplemented the adult bovine serum with amino acids, glucose, and pyruvate to match levels

found in RPMI or DMEM. Levels of vitamins and micronutrients were added to adult bovine serum at the RPMI or DMEM concentration. Addition of RPMI nutrients (glucose, amino acids, vitamins and micronutrients) to adult bovine serum resulted in increased glutamine contribution to the TCA cycle in A549 cells (Fig. 3A). Addition of nutrients to adult bovine serum to levels found in either RPMI or DMEM also caused increased A549 sensitivity to CB-839 (Fig. 3B, Fig. 3 Supplement 1A). Thus, culturing cells in nutrient levels found in standard tissue culture media is sufficient to increase glutamine catabolism and dependence in these cells.

We next added different subsets of RPMI or DMEM nutrients to adult bovine serum to identify which nutrient(s) promote increased glutamine utilization and dependence. Addition of amino acids alone at RPMI levels to adult bovine serum increased glutamine contribution to the TCA cycle to the same extent as addition of the whole pool of all RPMI nutrients did (Fig. 3A). Addition of amino acids alone at RPMI levels also induced CB-839 sensitivity (Fig. 3B), as did addition of amino acids to DMEM levels (Fig. 3 Supplement 1A). We next sought to identify the amino acid(s) causing this increased use of glutamine. Because DMEM contains fewer amino acids, and causes the same phenotype as RPMI amino acids, we reasoned that the amino acids responsible must be present in DMEM. Therefore, we systematically determined CB-839 sensitivity of cells cultured in adult bovine serum supplemented with these amino acids lacking subsets that share common transport mechanisms (Hediger et al., 2013; Hyde et al., 2003). Adding the DMEM amino acid pool lacking serine, glycine, threonine and cystine to adult bovine serum failed to cause increased sensitivity of cells to CB-839, while omitting other subsets of amino acids had no effect on CB-839 sensitivity (Fig. 3 Supplement 1A). These data argue that one or more of these four amino acids is responsible for the phenotype. Serine, glycine, threonine or cystine were individually increased to DMEM levels in adult bovine serum containing DMEM levels of other amino acids. Only cystine addition triggered sensitivity to CB-839 (Fig. 3 Supplement 1B). Addition of cystine alone to adult bovine serum is sufficient to sensitize cells to CB-839 (Fig. 3B). Similarly, addition of cystine at RPMI levels to adult bovine

serum causes an increase in glutamine labeling of TCA cycle intermediates that is comparable to the labeling pattern observed in cells cultured in adult bovine serum containing levels of all nutrients found in RPMI (Fig. 3A). Cystine levels in adult plasma (~20-50 μM) are 4-10 fold lower than in DMEM or RPMI (~200 μM) (Table 1). These experiments demonstrate that high levels of cystine found in standard tissue culture formulations cause enhanced glutamine anaplerosis and dependence.

Cystine driven glutamine anaplerosis requires xCT/SLC7A11 expression

How might exogenous cystine regulate the contribution of glutamine carbon to the TCA cycle and drive glutamine dependence? Glutamine metabolism is linked to cystine metabolism via the x_c^- transporter system. This transporter system is composed of the transporter xCT (encoded by *SLC7A11*) and the chaperone 4F2hc/CD98 (encoded by *SLC3A2*), and together they mediate the exchange of glutamate for cystine across the plasma membrane (Lewerenz et al., 2013). We hypothesized that in the presence of high exogenous cystine, xCT-mediated transport of glutamate might deplete the intracellular glutamate/αKG pool, thus promoting glutamate regeneration from glutamine via glutaminase (Fig. 4A). To determine if xCT/*SLC7A11* was required for cystine induced glutamine anaplerosis and dependence, we generated A549 cells with shRNA-mediated stable knockdown of *SLC7A11*, where knockdown was or was not rescued by expression of an shRNA-resistant *SLC7A11* cDNA (Fig. 4B). The fate of [U-$^{13}C_5$]glutamine was traced in these cells cultured in adult bovine serum or adult bovine serum supplemented with RPMI levels of cystine. To quantify the extent to which cystine enhanced glutamine anaplerosis, we assessed the difference between normalized m+5 labeled αKG in adult bovine serum and in adult bovine serum with high cystine. We found that knockdown of *SLC7A11* substantially decreased the ability of cystine to potentiate glutamine anaplerosis, and that this effect was blunted by expression of the shRNA-resistant *SLC7A11* cDNA (Fig. 4C). Additionally, knockdown of *SLC7A11* with multiple hairpins (Fig. 4D) abrogated CB-839

sensitivity of A549 cells in adult bovine serum with RPMI levels of cystine (Fig. 4E). Thus, xCT/*SLC7A11* is necessary for cystine induced glutamine anaplerosis and dependence in A549 cells.

We next asked if xCT/*SLC7A11* expression influences cystine-induced glutamine anaplerosis across other human cancer cell lines. We traced [U-$^{13}C_5$]glutamine fate in a panel of human cell lines from cancers arising in multiple tissues and with multiple genetic drivers (Figure 4 Source Data). These cells were cultured in RPMI or RPMI with low (10 μM) cystine and the extent of glutamine anaplerosis determined as in Fig. 4C. We found a strong correlation between cystine-induced glutamine anaplerosis and xCT/*SLC7A11* mRNA expression reported by the Cancer Cell Line Encyclopedia (CCLE) (Barretina et al., 2012), suggesting that cystine levels and xCT/*SLC7A11* expression contribute to the prominent use of glutamine as a anaplerotic TCA cycle substrate in many cancer cells in culture (Fig. 4F).

Given that xCT/*SLC7A11* expression correlates with the ability of cystine to induce glutamine anaplerosis, we reasoned that xCT/*SLC7A11* expression might also be a determinant of glutaminase dependence in cancer cells. We compared reported CB-839 IC50 values (Gross et al., 2014) and xCT/*SLC7A11* mRNA expression levels from the CCLE for a panel of breast cancer cell lines (Fig. 4G and Figure 4 Source Data). Sensitive lines tend to have higher xCT/*SLC7A11* expression than resistant lines, suggesting that xCT/*SLC7A11* expression may contribute to a requirement for glutaminase in cultured cell lines.

We asked if increased xCT/*SLC7A11* expression in CB-839 resistant cell lines would be sufficient to cause cystine-induced glutamine anaplerosis and increase glutaminase inhibitor sensitivity. xCT/*SLC7A11* was expressed in three CB-839 resistant breast cancer cell lines, all of which had low baseline expression of this transport system: MCF7, MDA-MB-468 and AU565 (Fig. 4H). xCT/*SLC7A11* expression increased the incorporation of glutamine carbon into TCA cycle intermediates in the presence of RPMI levels of cystine in all three cell lines (Fig. 4I). xCT/*SLC7A11* expression also potentiated CB-839 sensitivity when these cells are cultured in

RPMI, but not RPMI with 10μM cystine (Fig. 4J and Figure 4 Supplement 1). These results demonstrate that xCT/*SLC7A11* is necessary and sufficient for increased glutamine anaplerosis and glutamine addiction in the presence of high levels of extracellular cystine.

Low environmental cystine availability limits glutamine anaplerosis in vivo

Lastly, we asked whether the relatively low level of cystine available *in vivo* could limit tumor glutamine anaplerosis of even xCT/*SLC7A11* expressing tumors. To ask this, we sought to increase cystine availability in A549 tumor bearing mice and monitor glutamine carbon incorporation into metabolites in these tumors. We found that an oral dose of 2.4 g/kg cystine could raise plasma cystine levels in mice from ~15 μM to ~70 μM for at least 4h (Fig. 5A). We next administered cystine and [U-$^{13}C_5$]glutamine to A549 tumor bearing mice to determine if cystine administration would increase glutamine anaplerosis. Technical limitations prevented us from administering cystine orally to mice surgically prepared for long-term glutamine infusion as performed in Fig. 1B; therefore, [U-$^{13}C_5$]glutamine was administered to tumor bearing mice via multiple bolus intravenous injections 30 minutes after cystine dosing. While this technique does not allow us to assess steady state contribution of glutamine into the TCA cycle, glutamine intravenous bolus injections have previously been used to detect changes in tumor glutamine utilization (Elgogary et al., 2016; Lane et al., 2015; Tardito et al., 2015; Yuneva et al., 2012). Additionally, if xCT/*SLC7A11* expression increases glutamate efflux and turnover rate in the presence of cystine, then kinetic labeling of glutamate, which will be captured by bolus glutamine labeling, will be higher in the presence of exogenous cystine. Terminal [U-$^{13}C_5$]glutamine plasma enrichment was similar in cystine-treated and untreated animals, while cystine-treated animals had substantially higher plasma cystine concentrations (Fig. 5B). Labeling of glutamine, glutamate and aKG from [U-$^{13}C_5$]glutamine in tumors was significantly higher in cystine treated mice, consistent with increased glutamine catabolism in these tumors (Fig. 5B). Relative to tumor [U-$^{13}C_5$]glutamine enrichment, ^{13}C-labeling of glutamate and aKG

was also higher in cystine treated mice (Fig. 5C). These results suggest that low cystine levels *in vivo* limit glutamine anaplerosis and that increasing cystine levels in tumors can cause increased glutamine carbon contribution to TCA cycle metabolism.

Discussion

Coincidence of xCT/SLC7A11 expression and high environmental cystine contribute to increased glutamine metabolism

Environmental differences between *in vitro* culture conditions and tumors *in vivo* can lead to differential reliance on glutamine anaplerosis, causing some cells to be addicted to glutamine catabolism *in vitro*. We found that non-physiological cystine levels in tissue culture can explain many of the differences in glutamine metabolism between lung cancer cells *in vitro* and in tumors. The glutamate/cystine antiporter xCT/*SLC7A11* is necessary for the observed cystine-induced glutamine anaplerosis in A549 cells. Thus, high levels of extracellular cystine and the cellular capacity to secrete glutamate in exchange for cystine cooperate to increase glutamine anaplerosis in these cells.

Increased glutamate secretion in the presence of cystine increases intracellular glutamate turnover, which in turn will increase the kinetic rate of glutamine label incorporation into both glutamate and TCA cycle intermediates. However, there are multiple carbon sources that can contribute to the pool of TCA cycle metabolites, raising the question of why increased glutamate secretion also results in increased steady-state anaplerotic contribution of glutamine carbon relative to other nutrients. The enzymology of glutaminase suggests one potential explanation. GLS1 activity is strongly inhibited by glutamate (Cassago et al., 2012; Curthoys and Watford, 1995) suggesting that the drop in intracellular glutamate driven by high cystine could raise glutaminase activity and increase glutamine contribution to the TCA cycle relative to other pathways. Thus, it could be the action of non-physiological cystine concentrations

constantly depleting the intracellular glutamate pool that causes glutamine anaplerosis to become dominant.

xCT/*SLC7A11* expression correlates with the ability of cystine to increase glutamine anaplerosis in a panel of cell lines derived from tumors of different oncogenotype and tissue of origin (Fig. 4F). This argues that xCT/*SLC7A11* expression may be necessary for environmental cystine to enhance glutamine anaplerosis regardless of tumor type, and is not a phenomenon limited to NSCLC and A549 cells. Indeed, examination of panels of human breast cancer cell lines have found that xCT/*SLC7A11* promotes glutamate secretion, providing further evidence that xCT/*SLC7A11* can promote glutamine catabolism in cell types beyond NSCLC (Briggs et al., 2016; Timmerman et al., 2013). Collectively, these experiments suggest that glutaminase dependence in culture for many cancer cells derived from various tumor types will be strongly influenced by both environmental cystine and xCT/*SLC7A11* expression.

Therapeutic implications of tissue cystine levels and their relationship to glutamine anaplerosis

These findings have clear implications for the clinical use of glutaminase inhibitors that are being evaluated in trials to treat a variety of tumor types (https://clinicaltrials.gov/ct2/show/NCT02071862). First, assessing xCT/*SLC7A11* expression may help identify patients likely to benefit from these drugs. While many cancer cells are considered to be glutamine addicted, not every cancer cell line requires glutamine for proliferation *in vitro* (Cetinbas et al., 2016; Cheng et al., 2011; Gross et al., 2014; Timmerman et al., 2013; van den Heuvel et al., 2012). Glutamine dependence has been linked to various oncogenes including *MYC* (Gao et al., 2009; Wise et al., 2008), *RAS* (Son et al., 2013), *IDH* (Matre et al., 2014; Seltzer et al., 2010) and hormone receptor status in breast cancers (Gross et al., 2014). However, the genetic and biochemical basis for glutamine dependence remains poorly understood. Thus, understanding the underlying factors that cause increased reliance on

glutamine is essential for identifying patients that would likely benefit from clinical glutaminase inhibitors. Identification of high xCT/*SLC7A11* expression as a marker for glutaminase inhibitor sensitivity may be useful to identify patients that are more likely to benefit from glutaminase inhibitor therapy regardless of genotype. Functional examination of glutamate/cystine exchange by tumor cells using imaging techniques such as xCT-specific PET probes (Baek et al., 2012) may also be helpful in selecting tumors that are dependent on glutamine metabolism.

xCT/*SLC7A11* expression is known to be governed by the antioxidant response transcription factor NRF2 (Sasaki et al., 2002). Interest in modulating the antioxidant response pathway has led to the development of a number of NRF2-activating compounds, some of which are already in clinical use (Davies et al., 2016; Gao et al., 2014; Magesh et al., 2012). In addition, beyond the use of xCT/*SLC7A11* expression as a marker for glutaminase inhibitor responsiveness, raising tumor cystine levels might also be a way to induce or enhance glutamine addiction. We found that raising tissue cystine levels can increase glutamine anaplerosis in tumors. Therefore, co-administration of cystine with glutaminase inhibitors may enhance responses to glutaminase inhibitors. Oral cystine administration can be effective to raise plasma cystine levels in humans (Morin et al., 1971), arguing that this strategy may be applicable to treating patients.

Tissue culture systems that reflect nutrient availability in vivo can be more representative models of tumor metabolism

Eagle's medium and RPMI were formulated to identify the minimal set of nutrients required for mammalian cancer cells and leukocytes to rapidly proliferate (Eagle, 1955; Moore et al., 1967), not to match physiological levels of nutrients available *in vivo*. Thus, these media lack certain nutrients available to tumors *in vivo* and also contain other nutrients in excess to what is found in blood. Several studies examining tumor metabolism in mice and humans have suggested that the way nutrients are used in tumors can be different from what is observed in

cell culture. While increased glucose consumption and lactate secretion observed in most cells in culture is also observed in tumors (Davidson et al., 2016; Hensley et al., 2016; Marin-Valencia et al., 2012; Mashimo et al., 2014; Sellers et al., 2015; Tardito et al., 2015), glutamine oxidation and anaplerosis can differ between both lung and glial tumors and cell lines derived from these tumors in culture (Davidson et al., 2016; Marin-Valencia et al., 2012; Tardito et al., 2015). Thus, standard tissue culture can cause some aspects of central carbon metabolism to be misrepresented and the identification of media that better model the environmental conditions in tumors may facilitate better understanding of cancer metabolism.

Previous studies have suggested that altering tissue culture media to better reflect levels of amino acids found in human plasma can allow more accurate modeling of tissue metabolism (Schug et al., 2015; Tardito et al., 2015). Culturing glioblastoma cells in serum-like medium (SMEM) results in decreased glutamine utilization and a requirement to net produce glutamine from other carbon sources, similar to what is observed in glioblastoma *in vivo* (Tardito et al., 2015). The differences between SMEM and standard media formulations that elicited this difference is unknown, but the fact that culturing cells in media with more physiological cystine levels resulted in a change in glutamine metabolism is consistent with our findings.

In culture systems, the bulk of TCA cycle carbon can be accounted for from glucose and glutamine. However, the sources of anaplerotic TCA cycle carbon in tumors are not fully understood despite the increased contribution of glucose anaplerosis in some settings (Davidson et al., 2016; Hensley et al., 2016; Sellers et al., 2015). Adult bovine serum differs from standard media in levels of many nutrients. Thus, additional nutritional differences beyond amino acids may contribute to why glutamine metabolism of A549 cells in serum more closely mimics A549 tumors *in vivo* and suggests factors other than cystine levels might be involved. Supporting this hypothesis, addition of cystine to adult bovine serum increases A549 incorporation of glutamine carbon into the TCA cycle, but not to the same levels observed when the same cells are cultured in RPMI (Fig. 3A). Additionally, A549 cells grown in adult bovine

serum are also more resistant to CB-839 than A549 cells grown in RPMI with low levels of cystine (10μM) (Fig. 3B). These results suggest that alternative anaplerotic carbon source(s) are available in adult bovine serum that contribute to further glutaminase independence. Identification of what contributes to the TCA cycle in serum may yield new insight into the anaplerotic carbon sources used by cells *in vivo*.

Beyond the contribution of oncogenic mutations to reprogramming cellular metabolism, environment also plays a fundamental role in determining the metabolic program of cancer cells. We find that environmental cystine level is one variable that can alter how nutrients are used by cancer cells. Many studies aim to identify the set of genes required for cancer cell proliferation, with the goal of identifying novel therapeutic targets (Hart et al., 2015; Shalem et al., 2014; Wang et al., 2017). Based on our results, selection of media conditions will be essential to maximize the *in vivo* relevance of targets identified by screens to find metabolic gene vulnerabilities. Our results motivate further studies to characterize the nutritional content of the tumor microenvironment, and development of tissue culture systems to propagate and study cells under such conditions, as this may help translate metabolic dependencies of cancer cell lines into better cancer therapies.

Figure Legends

Figure 1 Decreased use of glutamine for TCA cycle anaplerosis by A549 cells in tumors, and when cultured in adult bovine serum, compared to RPMI. (A) Diagram detailing how uniformly-labeled glutamine ([U-$^{13}C_5$]glutamine) can be metabolized to generate labeled glutamate, aspartate and TCA cycle intermediates via oxidative metabolism. (B) *Left* Plasma fractional labeling of fully labeled glutamine (m+5) in A549 tumor bearing mice following a 6h infusion of [U-$^{13}C_5$]glutamine (n=3). *Right* Intratumoral fractional labeling of glutamine (m+5), glutamate (m+5), α-ketoglutarate (m+5), fumarate (m+4), malate (m+4), aspartate (m+4) and citrate (m+4) following a 6h infusion of [U-$^{13}C_5$]glutamine (n=3). (C) M+5 fractional labeling of glutamine,

glutamate and α-ketoglutarate, and m+4 fractional labeling of fumarate, malate, aspartate and citrate for A549 cells cultured for 8h in RPMI or adult bovine serum with [U-$^{13}C_5$]glutamine added to ~33% enrichment (n=3). (D) Proliferation rate of A549 cells cultured in RPMI or adult bovine serum with vehicle (DMSO) or 1 μM CB-839 (n=3) as indicated. For all panels, the values represent the mean and the error bars represent ± SEM.

Figure 1 Source Data Mass isotopomer distributions for all metabolites analyzed by GC-MS in Figure 1.

Figure 1 Supplement 1 Glutamine labeling of metabolites in A549 cells cultured in adult bovine serum reaches isotopic steady state by 8 hours. M+5 fractional labeling of glutamine, glutamate and α-ketoglutarate, and m+4 labeling of fumarate, malate, aspartate and citrate for A549 cells cultured for 8h or 24h in adult bovine serum with [U-$^{13}C_5$]glutamine added to ~33% enrichment (n=3) is shown. The values represent the mean and the error bars represent ± SEM.

Figure 1 Supplement 1 Source Data Mass isotopomer distributions for all metabolites analyzed by GC-MS in Figure 1 Supplement 1.

Figure 1 Supplement 2 Decreased glutamine anaplerosis is not unique to serum or bovine derived blood products. M+5 fractional labeling of glutamine, glutamate and α-ketoglutarate, and m+4 labeling of fumarate, malate, aspartate and citrate for A549 cells cultured for 8h in RPMI, adult bovine serum, adult heparinized plasma or adult human serum with [U-$^{13}C_5$]glutamine added to ~33% enrichment (n=3). The values represent the mean and the error bars represent ± SEM.

Figure 1 Supplement 2 Source Data Mass isotopomer distributions for all metabolites analyzed by GC-MS in Figure 1 Supplement 2.

Figure 2 Differences in the small molecule (<3.5 kDa) fraction between RPMI and adult bovine serum account for differences in glutamine anaplerosis and sensitivity to glutaminase inhibition. (A) Diagram detailing the generation of *top* 'Adult bovine serum → RPMI' and *bottom* 'RPMI → adult bovine serum'. To make each dialyzed medium, 210 mL of RPMI or adult bovine serum was dialyzed twice against 4 L of adult bovine serum or RPMI respectively using 70 mL capacity 3.5 kDa cutoff dialysis cassettes. (B) M+5 fractional labeling of glutamine, glutamate and α-ketoglutarate, and m+4 labeling of fumarate, malate, aspartate and citrate for A549 cells cultured for 8h in 'Adult bovine serum → RPMI' and 'RPMI → adult bovine serum' with [U-$^{13}C_5$]glutamine added to each media at ~33% enrichment (n=3). (C) Proliferation rates of A549 cells cultured in RPMI, adult bovine serum, 'RPMI → adult bovine serum', 'Adult bovine serum → RPMI' with vehicle (DMSO) or 1 μM CB-839 (n=3). For all panels, the values represent the mean and the error bars represent ± SEM.

Figure 2 Source Data Mass isotopomer distributions for all metabolites analyzed by GC-MS in Figure 2.

Figure 2 Supplement 1 Differences in the small molecule (<3.5 kDa) fraction between DMEM and adult bovine serum account for differences in glutamine anaplerosis and sensitivity to glutaminase inhibition. (A) Diagram detailing the generation of *top* 'Adult bovine serum → DMEM' and *bottom* 'DMEM → adult bovine serum'. To make each dialyzed medium, 210 mL of DMEM or adult bovine serum was dialyzed twice against 4 L of adult bovine serum or DMEM respectively using 70 mL capacity 3.5 kDa cutoff dialysis cassettes. (B) M+5 fractional labeling of glutamine, glutamate and α-ketoglutarate, and m+4 labeling of fumarate, malate, aspartate

and citrate for A549 cells cultured for 8h in DMEM, adult bovine serum and 'Adult bovine serum → DMEM' with [U-$^{13}C_5$]glutamine added to each media at ~33% enrichment (n=3). (C) Proliferation rates of A549 cells cultured in DMEM, adult bovine serum, 'DMEM → adult bovine serum', 'Adult bovine serum → DMEM' with vehicle (DMSO) or 1 μM CB-839 (n=3). For all panels, the values represent the mean and the error bars represent ± SEM.

Figure 2 Supplement 1 Source Data Mass isotopomer distributions for all metabolites analyzed by GC-MS in Figure 2 Supplement 1.

Figure 3 High levels of cystine enhance glutamine anaplerosis and potentiate the effects of the glutaminase inhibitor CB-839 (A) M+5 fractional labeling of glutamine, glutamate and α-ketoglutarate, and m+4 labeling of fumarate, malate, aspartate and citrate is shown for A549 cells cultured for 8h in RPMI, adult bovine serum, adult bovine serum with RPMI nutrient levels, adult bovine serum with RPMI amino acid levels and adult bovine serum with 208 μM cystine added (RPMI cystine levels). Each medium included [U-$^{13}C_5$]glutamine added to ~33% enrichment (n=3). (B) The proliferation of A549 cells cultured in the same media defined in (A) and RPMI containing 10 μM cystine with vehicle (DMSO) or 1 μM CB-839 as indicated (n=3). For all panels, the values represent the mean and the error bars represent ± SEM.

Figure 3 Source Data Mass isotopomer distributions for all metabolites analyzed by GC-MS in Figure 3.

Figure 3 Supplement 1 Identification of cystine as the metabolite in standard culture media that potentiates the glutaminase inhibitor CB-839. (A) A549 cells were cultured in adult bovine serum with DMEM nutrient levels, adult bovine serum with DMEM amino acid levels and adult bovine serum with DMEM amino acid levels, but without supplementation of the amino acids indicated

by their standard single letter code in each column. For each medium, the proliferation rate for cells cultured in the presence of vehicle (DMSO) or 1 μM CB-839 is shown (n=3). (B) A549 cells were cultured in adult bovine serum, adult bovine serum with DMEM amino acid levels, adult bovine serum with all DMEM amino acids supplemented except serine, glycine, threonine and cystine, or the previous medium supplemented with DMEM levels of serine, glycine, threonine or cystine added individually as indicated. For each medium, the proliferation rate for cells cultured in the presence of vehicle (DMSO) or 1 μM CB-839 is shown (n=3). For all panels, the values represent the mean and the error bars represent ± SEM.

Figure 4 The cystine/glutamate antiporter xCT/*SLC7A11* is necessary and sufficient for cystine induced glutamine anaplerosis and CB-839 sensitivity. (A) System x_c^- is a plasma membrane antiporter composed of two polypeptides, xCT (encoded by *SLC7A11*) and 4F2hc/CD98 (encoded by *SLC3A2*), that exchanges intracellular glutamate for extracellular cystine. (B) A549 cells were infected with lentiviruses encoding a *SLC7A11* targeting shRNA or a control shRNA targeting GFP as indicated. These cells were then infected with retroviruses expressing either shRNA resistant *SLC7A11* cDNA or empty vector (E.V.) as indicated. Shown is an immunoblot analysis of these modified cell lines for xCT protein expression with vinculin as a loading control. (C) The four cell lines from (B) were cultured for 8h in adult bovine serum or adult bovine serum with 208 μM cystine. Each medium included [U-$^{13}C_5$]glutamine added to ~33% enrichment (n=3). M+5 fractional labeling of α-ketoglutarate and glutamine for each cell line in each condition was determined. Shown is the difference in m+5 fractional label of α-ketoglutarate (normalized to m+5 fractional enrichment of glutamine) between adult bovine serum with 208 μM cystine and adult bovine serum. We define this as the 'cystine induced increase of glutamine contribution to αKG'. (D) Immunoblot analysis of A549 cells infected with lentiviruses encoding *SLC7A11* targeting shRNAs or a control shRNA targeting GFP as indicated. (E) Proliferation rates of cell lines from (D) cultured in adult bovine serum with 208 μM cystine with vehicle

(DMSO) or 1μM CB-839 is shown (n=3). (F) Multiple cell lines (see Figure 4 source data for identity of cell lines) were cultured for 8h in RPMI or RPMI with 10μM cystine. Each medium included [U-$^{13}C_5$]glutamine added to ~33% enrichment (n=2-3). M+5 fractional labeling of α-ketoglutarate and glutamine for each cell line in each condition was determined. Shown is 'cystine induced increase of glutamine contribution to αKG' defined as the difference of m+5 fractional label of α-ketoglutarate (normalized to m+5 fractional enrichment of glutamine) between RPMI and RPMI with 10μM cystine for a given cell line. This term is plotted against *SLC7A11* mRNA expression data obtained from the cancer cell line encyclopedia (CCLE) (Barretina et al., 2012). (G) *SLC7A11* mRNA expression data from the CCLE is shown for breast cancer cell lines reported to be CB-839 resistant (IC50 > 1 μM) or CB-839 sensitive (IC50 < 1 μM) (Gross et al., 2014). Difference in *SLC7A11* expression between the two groups was tested by two-tailed unpaired t-test with the p value for significance shown. (H) Indicated cell lines were infected with lentiviruses encoding *SLC7A11* cDNA or empty vector (E.V.). Shown is an immunoblot analysis of xCT protein expression for these modified cell lines with vinculin expression presented as a loading control. (I) Cystine induced increase of glutamine contribution to αKG was determined as in (F) for the cell lines described in (H). (J) Proliferation rates for MCF7 cells without (E.V.) or with SLC7A11 expression cultured in RPMI or RPMI with 10μM cystine in the presence of vehicle (DMSO) or 1μM CB-839 as indicated. For all panels, values represent the mean and the error bars represent ± SEM.

Figure 4 Source Data Mass isotopomer distributions for all metabolites analyzed by GC-MS in Figure 4. Cell line identity and *SLC7A11* mRNA expression level for cell lines analyzed in 4F. Cell line identity and CB-839 sensitivity for cell lines analyzed in 4G.

Figure 4 Supplement 1 Overexpression of xCT/*SLC7A11* causes cystine-induced CB-839 sensitivity for MDA-MB-468 and AU565 breast cancer cell lines. Proliferation rates for MDA-MB-

468 and AU565 cell lines overexpressing *SLC7A11* or empty vector (from Fig. 4G) cultured in RPMI or RPMI with 10μM cystine in the presence of vehicle (DMSO) or 1μM CB-839 as indicated. The values represent the mean and the error bars represent ± SEM.

Figure 5 Raising cystine levels increases tumor glutamine anaplerosis *in vivo*. (A) nu/nu mice were treated with 2.4 g/kg cystine by oral gavage and plasma from these animals was serially collected at the indicated time points. Cystine concentration in plasma at each time point as determined by GC-MS is shown. (B) A549 tumor bearing mice were treated (n=4) or not (n=3) with oral cystine prior to three bolus [U-$^{13}C_5$]glutamine injections every 15 minutes. Plasma and tumor tissue was then harvested 15 minutes after the last injection (described in **Materials and Methods**). *Left* Enrichment of m+5 glutamine and cystine concentration in the plasma of these animals. *Right* Fractional labeling of glutamine (m+5), glutamate (m+5), α-ketoglutarate (m+5) in A549 tumor tissue. (C) Intratumoral glutamate (m+5) and α-ketoglutarate (m+5) labeling from (B) were normalized to tumor glutamine (m+5). For all panels, the values represent the mean and the error bars represent ± SEM.

Figure 5 Source Data Mass isotopomer distributions for all metabolites analyzed by GC-MS in Figure 5.

Table 1 Amino acid, glucose, pyruvate and lactate concentrations of media used in this study. Levels of the metabolites reported for human plasma (Blau, 2003) are also shown for reference.

Materials and Methods

Cell lines and culture

All cell lines used in this study were directly obtained from ATCC and DMSZ or were gifts from other laboratories. All cell lines not obtained directly from ATCC or DMSZ were STR

tested to confirm their identity prior to use (University of Arizona Genetics Core). All cell lines were regularly tested for mycoplasma contamination using the Mycoprobe mycoplasma detection kit (R&D Systems). All cells were cultured in a Heracell (Thermofisher) humidified incubators at 37 °C and 5% CO_2. Cell lines were routinely maintained in RPMI-1640 or DMEM (Cellgro) supplemented with 10% heat inactivated fetal bovine serum (Seradigm, Lot 120B14).

Media preparation and analysis

All stable isotope tracing and proliferation rate experiments were performed in RPMI or DMEM containing 10% heat inactivated fetal bovine serum (Seradigm, Lot 120B14) that was repeatedly dialyzed against saline (150 mM NaCl) using 3.5 kDa cutoff membranes (Thermofisher) to remove all small molecule metabolites from the serum.

Adult bovine serum (Sigma Aldrich, Lot 16A041), adult bovine heparinized plasma (Pel-freeze) and pooled adult human serum (Innovative Research, Lot 20211) were thawed at 37 °C for 2 h. and heat inactivated for 30 min. at 56 °C then filtered through a 0.22 µm filter prior to use or storage at -20 °C.

To analyze absolute concentrations of amino acids, pyruvate and lactate in adult bovine serum, adult heparinized plasma and adult human serum, 10 µL of the serum or plasma was added to 10 µL of isotopically labeled internal standards of amino acids (Cambrige Isotope Laboratory, MSK-A2-1.2, CLM-1822-H-PK, and CLM-8699-H-PK), pyruvate (Cambridge Isotope Laboratories, CLM-2440-PK) and lactate (Sigma Aldrich, 485926). These mixtures were then extracted in 600 µL of ice cold HPLC grade methanol, vortexed for 10 minutes, and centrifuged at 21 kg for 10 minutes. 450 µL of each extract was removed and dried under nitrogen gas and stored -80 °C until further analysis by GC-MS. Glucose concentration of serum or plasma was measured using a YSI-2900D Biochemistry Analyzer (Yellow Springs Instruments) according to the manufacturer's instructions.

To generate adult bovine serum containing added amino acids, stock amino acid mixtures were generated by adding individual amino acid powders (all obtained from Sigma Aldrich) at appropriate ratios in an electric blade coffee grinder (Hamilton Beach, 80365). The amino acids were then mixed using 10 pulses on the espresso setting. An appropriate amount of the amino acid mix was added to adult bovine serum, which was then sterilized using a 0.22 µm filter prior to use.

To prepare the dialyzed media 'Adult bovine serum → RPMI or DMEM', 210 mL of RPMI or DMEM was dialyzed twice overnight at 4 °C against 4 L of adult bovine serum using 70 mL 3.5 kDa cutoff dialysis cassettes (Thermofisher). For 'RPMI or DMEM → adult bovine serum', 210 mL of adult bovine serum was dialyzed against RPMI or DMEM as above. These media were sterilized using a 0.22 µm filter prior to use.

Generation of stable cDNA or shRNA expressing cell lines

Stable cDNA or shRNA expressing cell lines were generated by lentiviral or retroviral infection for 24 hours followed by selection in RPMI-1640 containing 1 µg/mL puromycin or 500 µg/mL hygromycin B. Mock infected cells were similarly selected, and selection was considered complete when no viable cells were detected in these mock infection controls. All virally manipulated cells were maintained under antibiotic selection at indicated concentrations until used in experimental assays.

Vectors

For reduction of xCT/*SLC7A11* expression, lentiviral pLKO human *SLC7A11* shRNA vectors (*SLC7A11* shRNA #1: TRCN0000288926 and *SLC7A11* shRNA #2: TRCN0000288927) containing the puromycin resistance gene were obtained from Sigma Aldrich. A pLKO vector targeting GFP was used as a control.

To rescue xCT/*SLC7A11* expression, cDNA encoding human *SLC7A11* was obtained from Origene. The cDNA was then PCR amplified and cloned into the HindIII and ClaI sites of retroviral vector pLHCX, which contains the hygromycin resistance gene (Clontech), allowing for CMV promoter driven expression of *SLC7A11*. Site directed mutagenesis (Hemsley et al., 1989) was performed to synonymously mutate the sequence of *SLC7A11* targeted by *SLC7A11* shRNA #1: TRCN0000288926 (CCCTGGAGTTATGCAGCTAAT) such that it would no longer be targeted by this shRNA (GCCCGGCGTGATGCAATTGAT).

To overexpress *SLC7A11*, *SLC7A11* cDNA was PCR amplified and ligated into the SalI and NotI sites of the vector pENTR4(no ccDB) (Addgene) (Campeau et al., 2009). LR Gateway recombination (Thermofisher) was used to clone the *SLC7A11* cDNA from pENTR4(no ccDB) into the expression vector pLenti CMV Puro DEST (w118-1) (Addgene) to allow for puromycin selectable CMV driven expression of *SLC7A11* (Campeau et al., 2009).

All vectors constructed for this study had the entire coding sequence confirmed by Sanger sequencing (Quintara Biosciences) prior to use.

Determination of cellular proliferation rates

Cellular proliferation rate in different media and drug conditions was determined as previously described (Sullivan et al., 2015). Briefly, cell lines proliferating in log phase in RPMI medium were trypsinized, counted and plated into 6 well dishes (Corning) in 2 mL of RPMI medium and incubated overnight. Initial seeding density was 20,000 cells/well for A549 cells, or 50,000 cells for MCF7, AU565 and MDA-MB-468 cells. The next day, a 6 well plate of cells was trypsinized and counted to provide a number of cells at the start of the experiment. Cells were then washed twice with 2 mL of phosphate buffered saline (PBS), and 8 mL of the indicated media premixed with indicated compounds or vehicles was added. This large volume of media was chosen to prevent severe nutrient depletion, especially when adding adult bovine serum medium. Cells were then trypsinized and counted 4 days after adding the indicated medias.

Proliferation rate was determined using the following formula: Proliferation rate in doublings/day = [Log2(Final Day 4 cell count/Initial Day 0 cell count)] / 4 days. Cells were counted using a Cellometer Auto T4 Plus Cell Counter (Nexcelom Bioscience).

Preparation of cell extracts and immunoblotting

For immunoblotting analysis, cell lines growing in log phase were trypsinized, counted and plated at a density of 400,000 cells/well of a 6 well dish. The following day, cells were washed with 2 mL of PBS and then lysed in 100 µL RIPA buffer [25 mM Tris-Cl, 150 mM NaCl, 0.5% sodium deoxycholate, 1% Triton X-100, 1x cOmplete protease inhibitor (Roche)]. Cells were scraped and the resulting lysate was clarified by centrifugation at 21 kg for 20 min. Protein concentration of the lysate was determined by BCA assay (Thermofisher). Lysates were resuspended at 2µg/µL in Laemmli SDS PAGE sample loading buffer (10% glycerol, 2% SDS, 60 mM Tris-Cl pH 6.8, 1% β-mercaptoethanol, 0.01% bromophenol blue) and denatured at 100 °C for 5 min.

Extracts (30 µg of protein) were resolved by SDS PAGE using 10% acrylamide gels running at 120 V until the dye front left the gel. After SDS-PAGE resolution, protein extracts were transferred to nitrocellulose using an iBlot semidry transfer system (Thermofisher). Membranes were subsequently incubated with primary antibody in Odyssey buffer (Licor Biosciences), washed, and incubated with IRDye-conjugated anti-mouse and anti-rabbit IgG secondary antibodies in Odyssey buffer with 0.1% Tween-20 and 0.02% SDS. Blots were imaged using an Odyssey infrared scanner (Licor Biosciences).

Antibodies and dilutions used in this study were: 1:1000 rabbit anti-xCT (Cell Signaling Technology, 12691S), 1:10000 mouse anti-Vinculin (Abcam, ab18058), 1:10000 IR680LT dye conjugated goat anti-rabbit IgG (Licor Biosciences, 925-68021), 1:10000 IR800 dye conjugated goat anti-mouse IgG (Licor Biosciences, 925-32210).

Cell culture isotopic labeling experiments and metabolite extraction

To determine steady state labeling of polar metabolites by glutamine in cultured cells, cell lines were seeded at an initial density of 200,000 cells/well in a 6 well dish in 2 mL of RPMI medium. Cells were incubated for 24 hours, and then washed twice with 2 mL of PBS. Cells were then incubated for 8 or 24 hours in the indicated media, to which [U-$^{13}C_5$]glutamine (Cambridge Isotope Laboratories, CLM-1822-H-PK) was added, such that the fractional enrichment of glutamine in the given medium would be ~33%.

Following the labeling period, media was aspirated from cells and the cells were rapidly washed in ~8 mL of ice cold saline. The saline was subsequently aspirated and 600 µL of ice cold methanol:water (4:1) was added. Cells were scraped on ice, and the resulting extracts were vortexed for 10 minutes, and centrifuged at 21 kg for 10 minutes. 450 µL of each extract was removed and dried under nitrogen gas and stored -80°C until further analysis.

Animal Studies

All experiments performed in this study were approved by the MIT Committee on Animal Care (IACUC). Nu/nu mice were purchased from Charles River (088) and housed on a 12-hour light and 12-hour dark cycle, with ad lib access to food and water. For subcutaneous xenograft studies, mice were injected with 2,000,000 A549 cells (suspended in a volume of 100 µL PBS) per site into the right and left flank.

Continuous infusions were performed as previously described (Davidson et al., 2016). 3-4 days prior to tracer studies, tumor-bearing mice underwent a surgery to implant a catheter into the jugular vein and were allowed to recover. Mice were infused with [U-$^{13}C_5$]glutamine at 3.7 mg/kg/min for 300 minutes. At the end of the infusion, mice were terminally anesthetized with sodium pentobarbital and blood collected via heart puncture. Tissues were rapidly collected, freeze-clamped in liquid nitrogen, and stored -80°C.

Repeated bolus intravenous injection tracer studies were performed as previously described (Lane et al., 2015; Yuneva et al., 2012). Tumor-bearing mice were orally administered a 2.4g/kg dose of L-cystine (Sigma Aldrich). Cystine was formulated as a 240 mg/mL suspension in 0.1% Tween 80 and 0.5% methylcellulose. Forty-five minutes after gavage, mice were lightly anesthetized using isofluorane and intravenously injected with 200 µL of [U-$^{13}C_5$]glutamine tracer (36.2 mg/ml dissolved in saline). These injections were performed a total of 3 times at 15 minute intervals. Forty-five minutes after the first injection (and 15 minutes after the last injection), animals were euthanized, blood collected via heart puncture, and relevant tissues rapidly collected and freeze-clamped in liquid nitrogen.

Tumor and plasma metabolite extraction

Frozen tissues were weighed (10-20mg) and pulverized using a cryomill (Retsch). Metabolites were extracted in 1.3mL chloroform:methanol:water (4:6:3), vortexed for 10 minutes, and centrifuged at 21 kg for 10 minutes. Polar metabolites were dried under nitrogen gas and stored -80°C until further analysis.

Blood collected from animals was immediately placed in EDTA-tubes (Sarstedt) and centrifuged to separate plasma. To analyze absolute concentrations of amino acids in the plasma, including cystine, 10 µL of plasma was added to 10 µL of a mixture of isotopically labeled amino acids of known concentrations (Cambridge Isotope Laboratories, MSK-A2-1.2). To analyze fractional enrichment of metabolites, 10 µL of plasma was diluted with 10 µL of water. Diluted plasma samples were extracted in 600 µL of ice cold HPLC grade methanol, vortexed for 10 minutes, and centrifuged at maximum speed for 10 minutes. 450 µL of each extract was removed and dried under nitrogen gas and stored -80 °C until further analysis.

Mass spectrometry analysis of polar metabolites

Polar metabolites were analyzed by GC-MS as described previously (Lewis et al., 2014). Dried and frozen metabolite extracts were derivitized with 16 µL MOX reagent (Thermofisher) for 60 min. at 37 °C. Samples were then derivitized with N-tertbutyldimethylsilyl-N-methyltrifluoroacetamide with 1% tert-butyldimethylchlorosilane (Sigma Aldrich) 30 min. at 60 °C. Following derivitization, samples were analyzed by GC-MS, using a DB-35MS column (Agilent Technologies) installed in an Agilent 7890A gas chromatograph coupled to an Agilent 5997B mass spectrometer. Helium was used as the carrier gas at a flow rate of 1.2 mL/min. One microliter of sample was injected in split mode (all samples were split 1:1) at 270 °C. After injection, the GC oven was held at 100 °C for 1 min. and increased to 300 °C at 3.5 °C/min. The oven was then ramped to 320 °C at 20°C/min. and held for 5 min. at this 320 °C.

The MS system operated under electron impact ionization at 70 eV and the MS source and quadrupole were held at 230 °C and 150 °C respectively. The detector was used in scanning mode, and the scanned ion range was 100–650 m/z. Mass isotopomer distributions were determined by integrating appropriate ion fragments for each metabolite (Lewis et al., 2014) using in-house software (Young et al., 2008) that corrects for natural abundance using previously described methods (Fernandez et al., 1996).

Acknowledgements

We thank all members of the Vander Heiden lab for many useful discussions and experimental advice. We also thank Caroline Lewis at the Whitehead Institute Metabolite Profiling Core for advice on GC-MS analysis of metabolites. CB-839 was a generous gift of Craig Thomas (NIH National Center for Advancing Translational Sciences). Several cell lines used in this study were generously provided by Alec Kimmelman (New York University) and David Sabatini (Whitehead Institute for Biomedical Research). We also thank the many thousands of citizens who continue to protest policies of the federal government that damage scientific institutions and practice in the United States. Their continued service to the American

scientific enterprise, which has made this work possible, is invaluable. This work was supported by grants to M.G.V.H. from the NIH (R01 CA168653, R01 CA201276, and P30CA1405141), the Lustgarten Foundation, SU2C, and the Ludwig Center at MIT. A.M. and L.V.D. were supported by NIH Ruth Kirschstein Fellowships, F32CA213810 and F32CA210421 respectively. D.Y.G. received support from T32GM007753. M.G.V.H. is a Howard Hughes Medical Institute Faculty Scholar.

References

Altman, B.J., Stine, Z.E., and Dang, C.V. (2016). From Krebs to clinic: glutamine metabolism to cancer therapy. Nat Rev Cancer *16*, 619-634.

Baek, S., Choi, C.M., Ahn, S.H., Lee, J.W., Gong, G., Ryu, J.S., Oh, S.J., Bacher-Stier, C., Fels, L., Koglin, N.*, et al.* (2012). Exploratory clinical trial of (4S)-4-(3-[18F]fluoropropyl)-L-glutamate for imaging xC- transporter using positron emission tomography in patients with non-small cell lung or breast cancer. Clin Cancer Res *18*, 5427-5437.

Barretina, J., Caponigro, G., Stransky, N., Venkatesan, K., Margolin, A.A., Kim, S., Wilson, C.J., Lehar, J., Kryukov, G.V., Sonkin, D.*, et al.* (2012). The Cancer Cell Line Encyclopedia enables predictive modelling of anticancer drug sensitivity. Nature *483*, 603-607.

Bhutia, Y.D., Babu, E., Ramachandran, S., and Ganapathy, V. (2015). Amino Acid transporters in cancer and their relevance to "glutamine addiction": novel targets for the design of a new class of anticancer drugs. Cancer Res *75*, 1782-1788.

Blau, N. (2003). Physician's guide to the laboratory diagnosis of metabolic diseases, 2nd edn (Berlin ; New York: Springer).

Brand, K. (1985). Glutamine and glucose metabolism during thymocyte proliferation. Pathways of glutamine and glutamate metabolism. Biochem J *228*, 353-361.

Brand, K., Leibold, W., Luppa, P., Schoerner, C., and Schulz, A. (1986). Metabolic alterations associated with proliferation of mitogen-activated lymphocytes and of lymphoblastoid cell lines: evaluation of glucose and glutamine metabolism. Immunobiology *173*, 23-34.

Briggs, K.J., Koivunen, P., Cao, S., Backus, K.M., Olenchock, B.A., Patel, H., Zhang, Q., Signoretti, S., Gerfen, G.J., Richardson, A.L.*, et al.* (2016). Paracrine Induction of HIF by Glutamate in Breast Cancer: EglN1 Senses Cysteine. Cell *166*, 126-139.

Campeau, E., Ruhl, V.E., Rodier, F., Smith, C.L., Rahmberg, B.L., Fuss, J.O., Campisi, J., Yaswen, P., Cooper, P.K., and Kaufman, P.D. (2009). A versatile viral system for expression and depletion of proteins in mammalian cells. PLoS One *4*, e6529.

Cassago, A., Ferreira, A.P., Ferreira, I.M., Fornezari, C., Gomes, E.R., Greene, K.S., Pereira, H.M., Garratt, R.C., Dias, S.M., and Ambrosio, A.L. (2012). Mitochondrial localization and

structure-based phosphate activation mechanism of Glutaminase C with implications for cancer metabolism. Proc Natl Acad Sci U S A *109*, 1092-1097.

Cetinbas, N.M., Sudderth, J., Harris, R.C., Cebeci, A., Negri, G.L., Yilmaz, O.H., DeBerardinis, R.J., and Sorensen, P.H. (2016). Glucose-dependent anaplerosis in cancer cells is required for cellular redox balance in the absence of glutamine. Sci Rep *6*, 32606.

Cheng, T., Sudderth, J., Yang, C., Mullen, A.R., Jin, E.S., Mates, J.M., and DeBerardinis, R.J. (2011). Pyruvate carboxylase is required for glutamine-independent growth of tumor cells. Proc Natl Acad Sci U S A *108*, 8674-8679.

Coloff, J.L., Murphy, J.P., Braun, C.R., Harris, I.S., Shelton, L.M., Kami, K., Gygi, S.P., Selfors, L.M., and Brugge, J.S. (2016). Differential Glutamate Metabolism in Proliferating and Quiescent Mammary Epithelial Cells. Cell Metab *23*, 867-880.

Cori, C.F., and Cori, G.T. (1925). The carbohydrate metabolism of tumors. II. Changes in the sugar, lactic acid, and co-combing power of blood passing through a tumor. Journal of Biological Chemistry *65*, 397-405.

Curthoys, N.P., and Watford, M. (1995). Regulation of glutaminase activity and glutamine metabolism. Annu Rev Nutr *15*, 133-159.

Davidson, S.M., Papagiannakopoulos, T., Olenchock, B.A., Heyman, J.E., Keibler, M.A., Luengo, A., Bauer, M.R., Jha, A.K., O'Brien, J.P., Pierce, K.A.*, et al.* (2016). Environment Impacts the Metabolic Dependencies of Ras-Driven Non-Small Cell Lung Cancer. Cell Metab *23*, 517-528.

Davies, T.G., Wixted, W.E., Coyle, J.E., Griffiths-Jones, C., Hearn, K., McMenamin, R., Norton, D., Rich, S.J., Richardson, C., Saxty, G.*, et al.* (2016). Monoacidic Inhibitors of the Kelch-like ECH-Associated Protein 1: Nuclear Factor Erythroid 2-Related Factor 2 (KEAP1:NRF2) Protein-Protein Interaction with High Cell Potency Identified by Fragment-Based Discovery. J Med Chem *59*, 3991-4006.

Daye, D., and Wellen, K.E. (2012). Metabolic reprogramming in cancer: unraveling the role of glutamine in tumorigenesis. Semin Cell Dev Biol *23*, 362-369.

DeBerardinis, R.J., and Chandel, N.S. (2016). Fundamentals of cancer metabolism. Sci Adv *2*, e1600200.

DeBerardinis, R.J., and Cheng, T. (2010). Q's next: the diverse functions of glutamine in metabolism, cell biology and cancer. Oncogene *29*, 313-324.

DeBerardinis, R.J., Mancuso, A., Daikhin, E., Nissim, I., Yudkoff, M., Wehrli, S., and Thompson, C.B. (2007). Beyond aerobic glycolysis: transformed cells can engage in glutamine metabolism that exceeds the requirement for protein and nucleotide synthesis. Proc Natl Acad Sci U S A *104*, 19345-19350.

Eagle, H. (1955). Nutrition needs of mammalian cells in tissue culture. Science *122*, 501-514.

Elgogary, A., Xu, Q., Poore, B., Alt, J., Zimmermann, S.C., Zhao, L., Fu, J., Chen, B., Xia, S., Liu, Y.*, et al.* (2016). Combination therapy with BPTES nanoparticles and metformin targets the metabolic heterogeneity of pancreatic cancer. Proc Natl Acad Sci U S A *113*, E5328-5336.

Fernandez, C.A., Des Rosiers, C., Previs, S.F., David, F., and Brunengraber, H. (1996). Correction of 13C mass isotopomer distributions for natural stable isotope abundance. J Mass Spectrom *31*, 255-262.

Gameiro, P.A., Yang, J.J., Metelo, A.M., Perez-Carro, R., Baker, R., Wang, Z.W., Arreola, A., Rathmell, W.K., Olumi, A., Lopez-Larrubia, P.*, et al.* (2013). In Vivo HIF-Mediated Reductive Carboxylation Is Regulated by Citrate Levels and Sensitizes VHL-Deficient Cells to Glutamine Deprivation. Cell Metabolism *17*, 372-385.

Gao, B., Doan, A., and Hybertson, B.M. (2014). The clinical potential of influencing Nrf2 signaling in degenerative and immunological disorders. Clin Pharmacol *6*, 19-34.

Gao, P., Tchernyshyov, I., Chang, T.C., Lee, Y.S., Kita, K., Ochi, T., Zeller, K.I., De Marzo, A.M., Van Eyk, J.E., Mendell, J.T.*, et al.* (2009). c-Myc suppression of miR-23a/b enhances mitochondrial glutaminase expression and glutamine metabolism. Nature *458*, 762-765.

Gross, M.I., Demo, S.D., Dennison, J.B., Chen, L., Chernov-Rogan, T., Goyal, B., Janes, J.R., Laidig, G.J., Lewis, E.R., Li, J.*, et al.* (2014). Antitumor activity of the glutaminase inhibitor CB-839 in triple-negative breast cancer. Mol Cancer Ther *13*, 890-901.

Hanahan, D., and Weinberg, R.A. (2011). Hallmarks of cancer: the next generation. Cell *144*, 646-674.

Hart, T., Chandrashekhar, M., Aregger, M., Steinhart, Z., Brown, K.R., MacLeod, G., Mis, M., Zimmermann, M., Fradet-Turcotte, A., Sun, S.*, et al.* (2015). High-Resolution CRISPR Screens Reveal Fitness Genes and Genotype-Specific Cancer Liabilities. Cell *163*.

Hediger, M.A., Clemencon, B., Burrier, R.E., and Bruford, E.A. (2013). The ABCs of membrane transporters in health and disease (SLC series): introduction. Mol Aspects Med *34*, 95-107.

Hemsley, A., Arnheim, N., Toney, M.D., Cortopassi, G., and Galas, D.J. (1989). A simple method for site-directed mutagenesis using the polymerase chain reaction. Nucleic Acids Res *17*, 6545-6551.

Hensley, C.T., Faubert, B., Yuan, Q., Lev-Cohain, N., Jin, E., Kim, J., Jiang, L., Ko, B., Skelton, R., Loudat, L.*, et al.* (2016). Metabolic Heterogeneity in Human Lung Tumors. Cell *164*, 681-694.

Hensley, C.T., Wasti, A.T., and DeBerardinis, R.J. (2013). Glutamine and cancer: cell biology, physiology, and clinical opportunities. J Clin Invest *123*, 3678-3684.

Hosios, A.M., Hecht, V.C., Danai, L.V., Johnson, M.O., Rathmell, J.C., Steinhauser, M.L., Manalis, S.R., and Vander Heiden, M.G. (2016). Amino Acids Rather than Glucose Account for the Majority of Cell Mass in Proliferating Mammalian Cells. Dev Cell *36*, 540-549.

Hyde, R., Taylor, P.M., and Hundal, H.S. (2003). Amino acid transporters: roles in amino acid sensing and signalling in animal cells. Biochem J *373*, 1-18.

Jain, M., Nilsson, R., Sharma, S., Madhusudhan, N., Kitami, T., Souza, A.L., Kafri, R., Kirschner, M.W., Clish, C.B., and Mootha, V.K. (2012). Metabolite profiling identifies a key role for glycine in rapid cancer cell proliferation. Science *336*, 1040-1044.

Krebs, H.A. (1935). Metabolism of amino-acids: The synthesis of glutamine from glutamic acid and ammonia, and the enzymic hydrolysis of glutamine in animal tissues. Biochem J *29*, 1951-1969.

Lane, A.N., Yan, J., and Fan, T.W. (2015). 13C Tracer Studies of Metabolism in Mouse Tumor Xenografts. Bio Protoc *5*.

Le, A., Lane, A.N., Hamaker, M., Bose, S., Gouw, A., Barbi, J., Tsukamoto, T., Rojas, C.J., Slusher, B.S., Zhang, H.*, et al.* (2012). Glucose-independent glutamine metabolism via TCA cycling for proliferation and survival in B cells. Cell Metab *15*, 110-121.

Lewerenz, J., Hewett, S.J., Huang, Y., Lambros, M., Gout, P.W., Kalivas, P.W., Massie, A., Smolders, I., Methner, A., Pergande, M.*, et al.* (2013). The cystine/glutamate antiporter system x(c)(-) in health and disease: from molecular mechanisms to novel therapeutic opportunities. Antioxid Redox Signal *18*, 522-555.

Lewis, C.A., Parker, S.J., Fiske, B.P., McCloskey, D., Gui, D.Y., Green, C.R., Vokes, N.I., Feist, A.M., Vander Heiden, M.G., and Metallo, C.M. (2014). Tracing compartmentalized NADPH metabolism in the cytosol and mitochondria of mammalian cells. Mol Cell *55*, 253-263.

Magesh, S., Chen, Y., and Hu, L. (2012). Small molecule modulators of Keap1-Nrf2-ARE pathway as potential preventive and therapeutic agents. Med Res Rev *32*, 687-726.

Marin-Valencia, I., Yang, C., Mashimo, T., Cho, S., Baek, H., Yang, X.L., Rajagopalan, K.N., Maddie, M., Vemireddy, V., Zhao, Z.*, et al.* (2012). Analysis of tumor metabolism reveals mitochondrial glucose oxidation in genetically diverse human glioblastomas in the mouse brain in vivo. Cell Metab *15*, 827-837.

Mashimo, T., Pichumani, K., Vemireddy, V., Hatanpaa, K.J., Singh, D.K., Sirasanagandla, S., Nannepaga, S., Piccirillo, S.G., Kovacs, Z., Foong, C.*, et al.* (2014). Acetate is a bioenergetic substrate for human glioblastoma and brain metastases. Cell *159*, 1603-1614.

Matre, P., Shariati, M., Velez, J., Qi, Y., Konoplev, S., Su, X.P., DiNardo, C.D., Daver, N., Majeti, R., Andreeff, M.*, et al.* (2014). Efficacy of Novel Glutaminase Inhibitor CB-839 in Acute Myeloid Leukemia. Blood *124*.

Mayers, J.R., and Vander Heiden, M.G. (2015). Famine versus feast: understanding the metabolism of tumors in vivo. Trends Biochem Sci *40*, 130-140.

Moore, G.E., Gerner, R.E., and Franklin, H.A. (1967). Culture of normal human leukocytes. JAMA *199*, 519-524.

Moreadith, R.W., and Lehninger, A.L. (1984). The pathways of glutamate and glutamine oxidation by tumor cell mitochondria. Role of mitochondrial NAD(P)+-dependent malic enzyme. J Biol Chem *259*, 6215-6221.

Morin, C.L., Thompson, M.W., Jackson, S.H., and Sass-Kortsak, A. (1971). Biochemical and genetic studies in cystinuria: observations on double heterozygotes of genotype I-II. J Clin Invest *50*, 1961-1976.

Patel, D., Menon, D., Bernfeld, E., Mroz, V., Kalan, S., Loayza, D., and Foster, D.A. (2016). Aspartate Rescues S-phase Arrest Caused by Suppression of Glutamine Utilization in KRas-driven Cancer Cells. J Biol Chem *291*, 9322-9329.

Pochini, L., Scalise, M., Galluccio, M., and Indiveri, C. (2014). Membrane transporters for the special amino acid glutamine: structure/function relationships and relevance to human health. Front Chem *2*, 61.

Sasaki, H., Sato, H., Kuriyama-Matsumura, K., Sato, K., Maebara, K., Wang, H., Tamba, M., Itoh, K., Yamamoto, M., and Bannai, S. (2002). Electrophile response element-mediated induction of the cystine/glutamate exchange transporter gene expression. J Biol Chem *277*, 44765-44771.

Schug, Z.T., Peck, B., Jones, D.T., Zhang, Q., Grosskurth, S., Alam, I.S., Goodwin, L.M., Smethurst, E., Mason, S., Blyth, K.*, et al.* (2015). Acetyl-CoA synthetase 2 promotes acetate utilization and maintains cancer cell growth under metabolic stress. Cancer Cell *27*, 57-71.

Sellers, K., Fox, M.P., Bousamra, M., 2nd, Slone, S.P., Higashi, R.M., Miller, D.M., Wang, Y., Yan, J., Yuneva, M.O., Deshpande, R.*, et al.* (2015). Pyruvate carboxylase is critical for non-small-cell lung cancer proliferation. J Clin Invest *125*, 687-698.

Seltzer, M.J., Bennett, B.D., Joshi, A.D., Gao, P., Thomas, A.G., Ferraris, D.V., Tsukamoto, T., Rojas, C.J., Slusher, B.S., Rabinowitz, J.D.*, et al.* (2010). Inhibition of glutaminase preferentially slows growth of glioma cells with mutant IDH1. Cancer Res *70*, 8981-8987.

Shalem, O., Sanjana, N.E., Hartenian, E., Shi, X., Scott, D.A., Mikkelsen, T.S., Heckl, D., Ebert, B.L., Root, D.E., Doench, J.G.*, et al.* (2014). Genome-Scale CRISPR-Cas9 Knockout Screening in Human Cells. Science *343*, 84-87.

Son, J., Lyssiotis, C.A., Ying, H.Q., Wang, X.X., Hua, S.J., Ligorio, M., Perera, R.M., Ferrone, C.R., Mullarky, E., Shyh-Chang, N.*, et al.* (2013). Glutamine supports pancreatic cancer growth through a KRAS-regulated metabolic pathway (vol 496, pg 101, 2013). Nature *499*.

Sullivan, L.B., Gui, D.Y., Hosios, A.M., Bush, L.N., Freinkman, E., and Vander Heiden, M.G. (2015). Supporting Aspartate Biosynthesis Is an Essential Function of Respiration in Proliferating Cells. Cell *162*, 552-563.

Tardito, S., Oudin, A., Ahmed, S.U., Fack, F., Keunen, O., Zheng, L., Miletic, H., Sakariassen, P.O., Weinstock, A., Wagner, A.*, et al.* (2015). Glutamine synthetase activity fuels nucleotide biosynthesis and supports growth of glutamine-restricted glioblastoma. Nat Cell Biol *17*, 1556-1568.

Timmerman, L.A., Holton, T., Yuneva, M., Louie, R.J., Padro, M., Daemen, A., Hu, M., Chan, D.A., Ethier, S.P., van 't Veer, L.J.*, et al.* (2013). Glutamine sensitivity analysis identifies the xCT antiporter as a common triple-negative breast tumor therapeutic target. Cancer Cell *24*, 450-465.

van den Heuvel, A.P., Jing, J., Wooster, R.F., and Bachman, K.E. (2012). Analysis of glutamine dependency in non-small cell lung cancer: GLS1 splice variant GAC is essential for cancer cell growth. Cancer Biol Ther *13*, 1185-1194.

Vander Heiden, M.G., and DeBerardinis, R.J. (2017). Understanding the Intersections between Metabolism and Cancer Biology. Cell *168*, 657-669.

Wang, J.B., Erickson, J.W., Fuji, R., Ramachandran, S., Gao, P., Dinavahi, R., Wilson, K.F., Ambrosio, A.L., Dias, S.M., Dang, C.V.*, et al.* (2010). Targeting mitochondrial glutaminase activity inhibits oncogenic transformation. Cancer Cell *18*, 207-219.

Wang, T., Yu, H., Hughes, N.W., Liu, B., Kendirli, A., Klein, K., Chen, W.W., Lander, E.S., and Sabatini, D.M. (2017). Gene Essentiality Profiling Reveals Gene Networks and Synthetic Lethal Interactions with Oncogenic Ras. Cell.

Warburg, O., Wind, F., and Negelein, E. (1927). The metabolism of tumors in the body. J Gen Physiol *8*, 519-530.

Wise, D.R., DeBerardinis, R.J., Mancuso, A., Sayed, N., Zhang, X.Y., Pfeiffer, H.K., Nissim, I., Daikhin, E., Yudkoff, M., McMahon, S.B.*, et al.* (2008). Myc regulates a transcriptional program that stimulates mitochondrial glutaminolysis and leads to glutamine addiction. P Natl Acad Sci USA *105*, 18782-18787.

Wise, D.R., and Thompson, C.B. (2010). Glutamine addiction: a new therapeutic target in cancer. Trends Biochem Sci *35*, 427-433.

Wise, D.R., Ward, P.S., Shay, J.E., Cross, J.R., Gruber, J.J., Sachdeva, U.M., Platt, J.M., DeMatteo, R.G., Simon, M.C., and Thompson, C.B. (2011). Hypoxia promotes isocitrate dehydrogenase-dependent carboxylation of alpha-ketoglutarate to citrate to support cell growth and viability. Proc Natl Acad Sci U S A *108*, 19611-19616.

Young, J.D., Walther, J.L., Antoniewicz, M.R., Yoo, H., and Stephanopoulos, G. (2008). An elementary metabolite unit (EMU) based method of isotopically nonstationary flux analysis. Biotechnol Bioeng *99*, 686-699.

Yuneva, M., Zamboni, N., Oefner, P., Sachidanandam, R., and Lazebnik, Y. (2007). Deficiency in glutamine but not glucose induces MYC-dependent apoptosis in human cells. J Cell Biol *178*, 93-105.

Yuneva, M.O., Fan, T.W., Allen, T.D., Higashi, R.M., Ferraris, D.V., Tsukamoto, T., Mates, J.M., Alonso, F.J., Wang, C., Seo, Y.*, et al.* (2012). The metabolic profile of tumors depends on both the responsible genetic lesion and tissue type. Cell Metab *15*, 157-170.

Figure 1

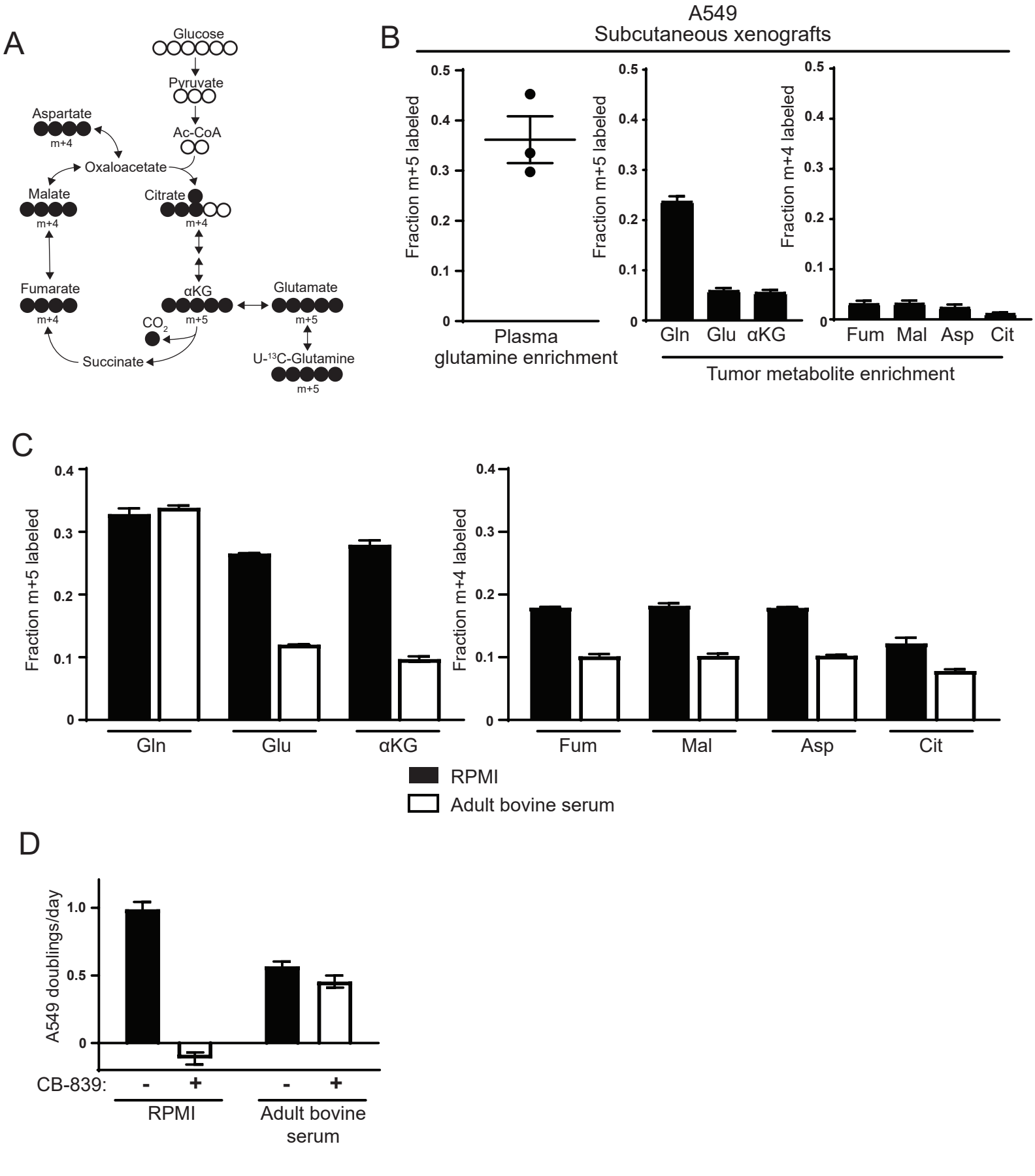

Figure 1 Supplement 1

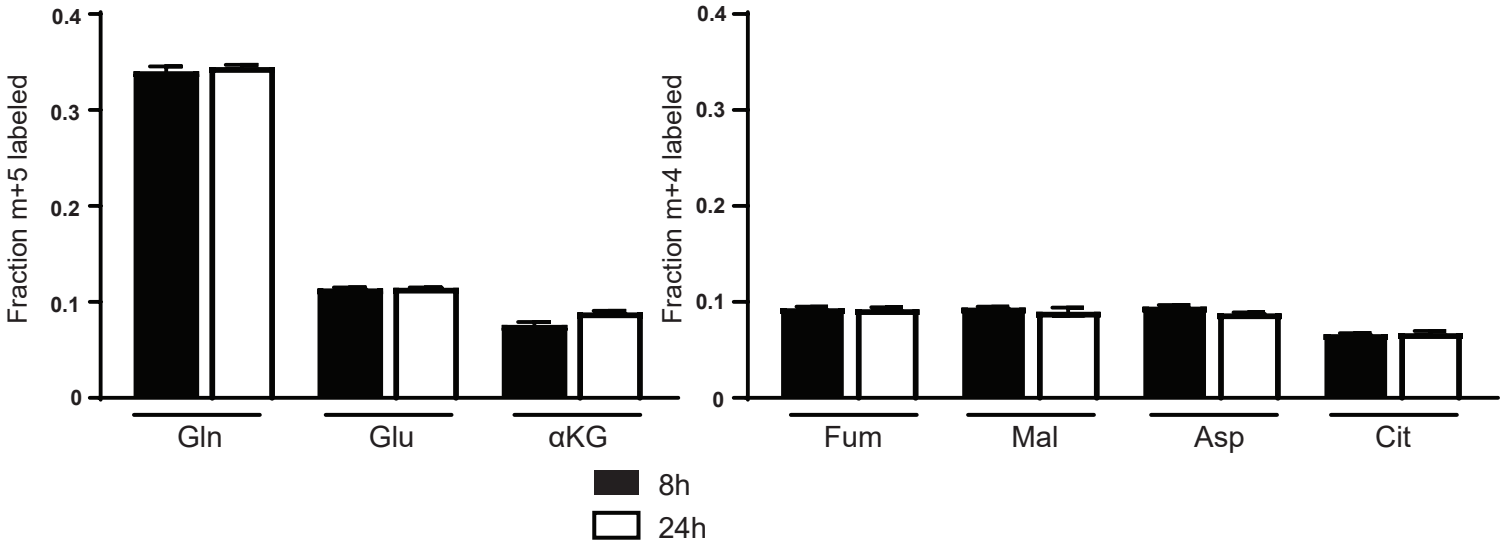

Figure 1 Supplement 2

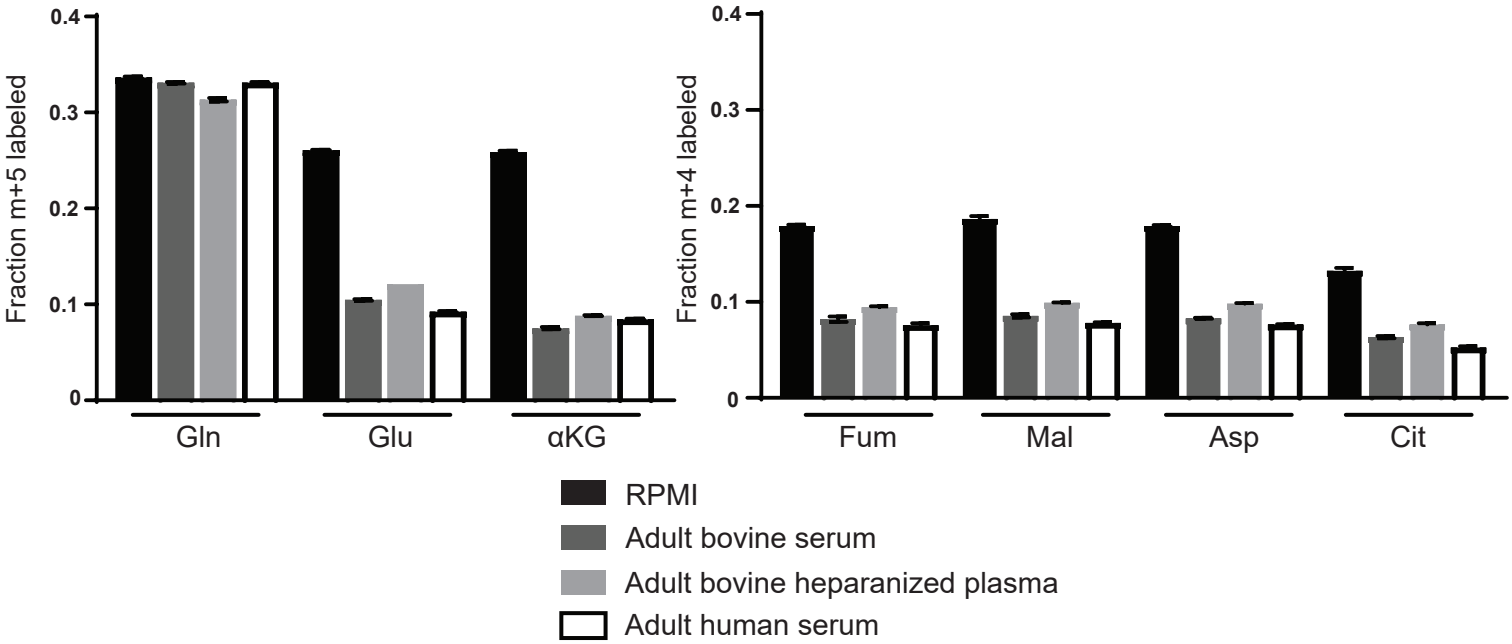

Figure 2

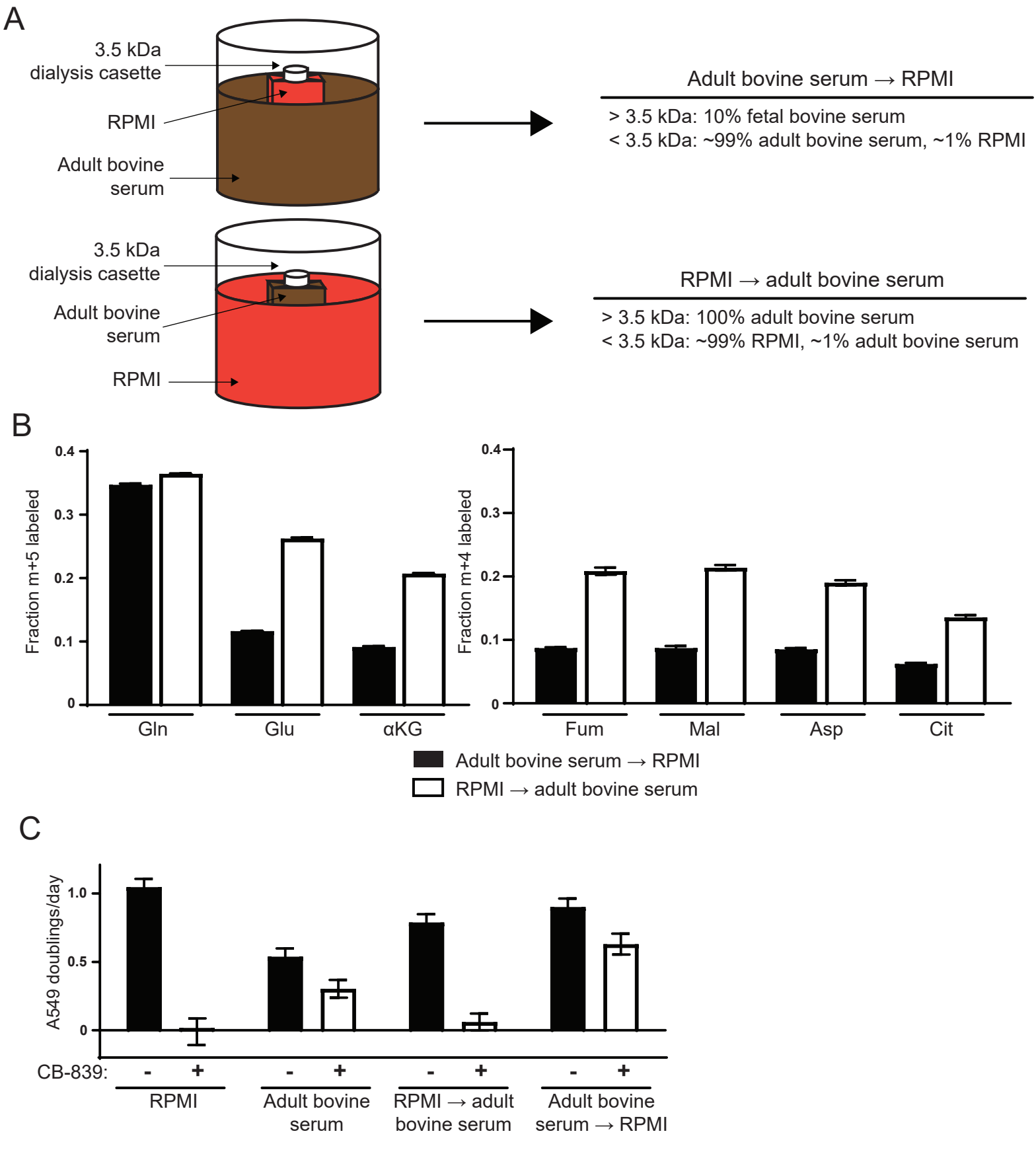

Figure 2 Supplement 1

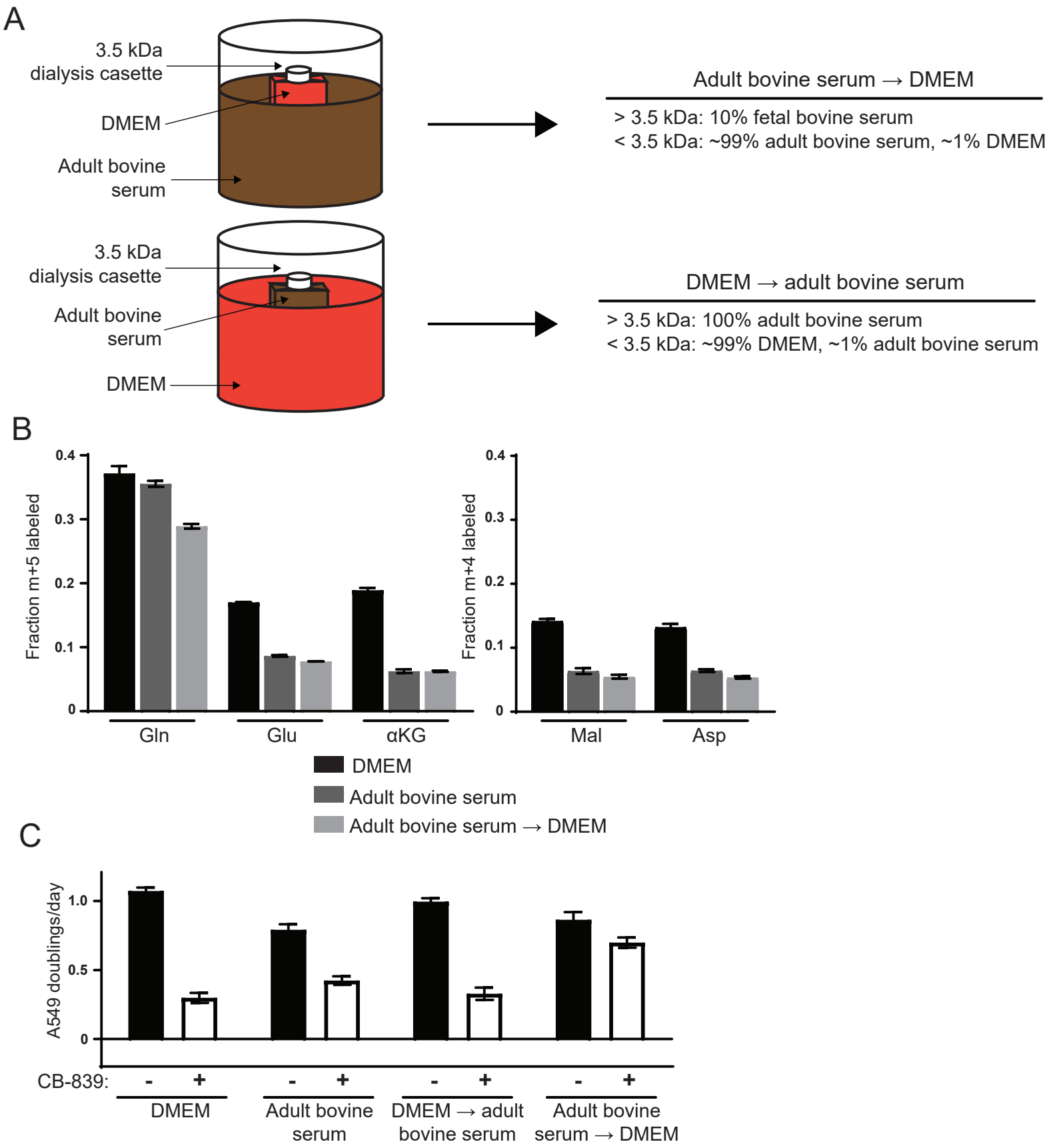

Figure 3

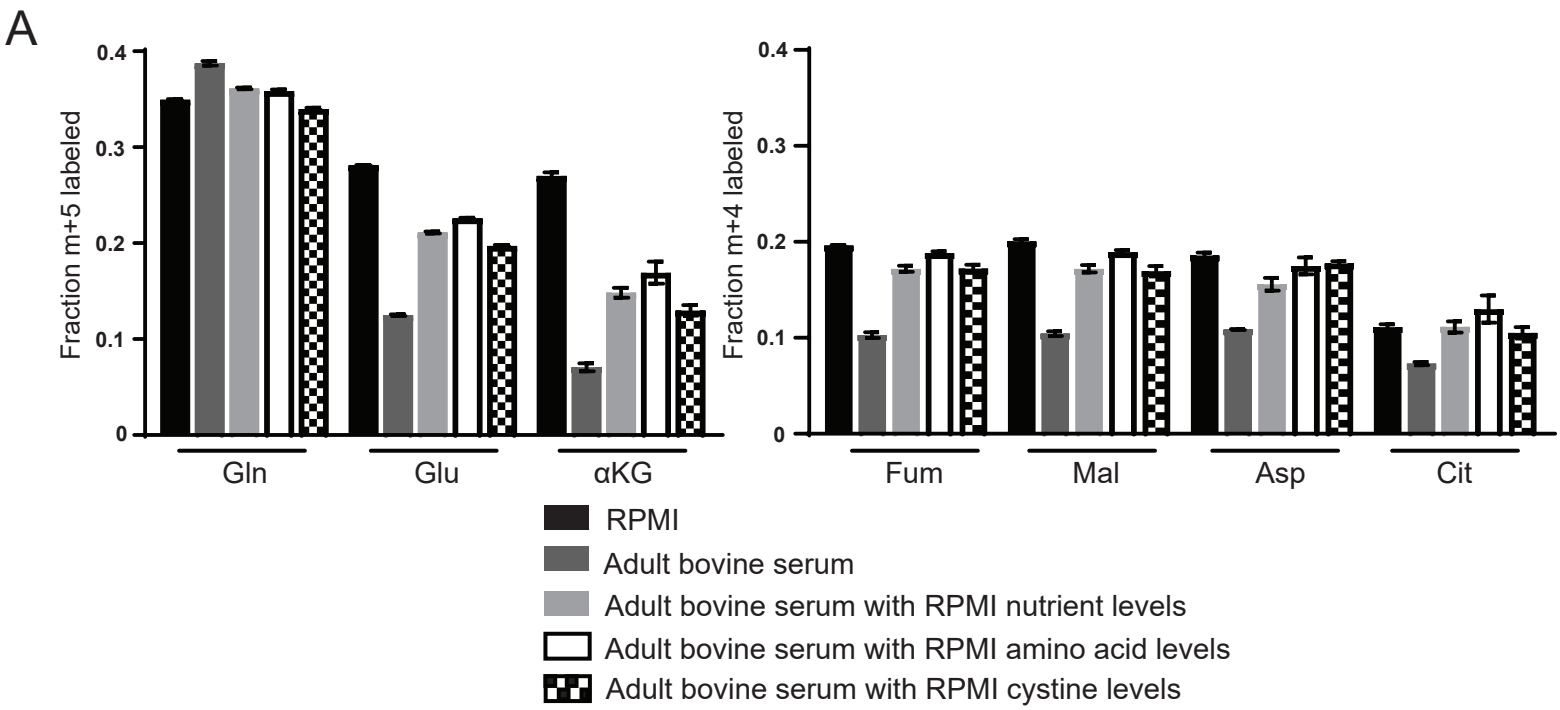

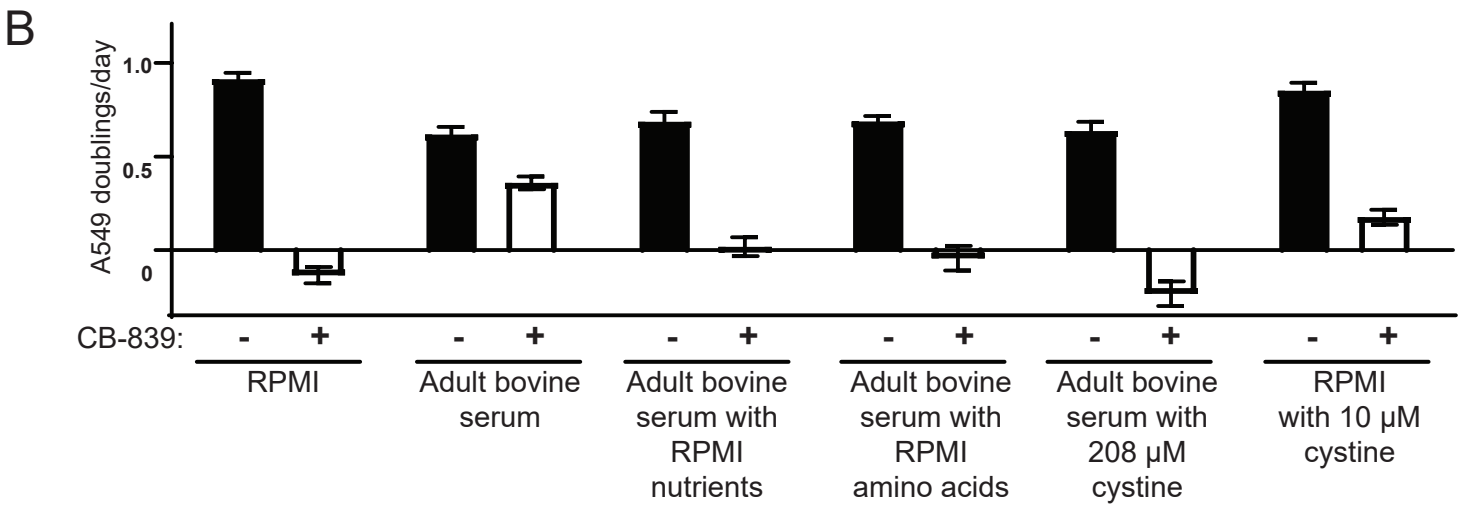

Figure 3 Supplement 1

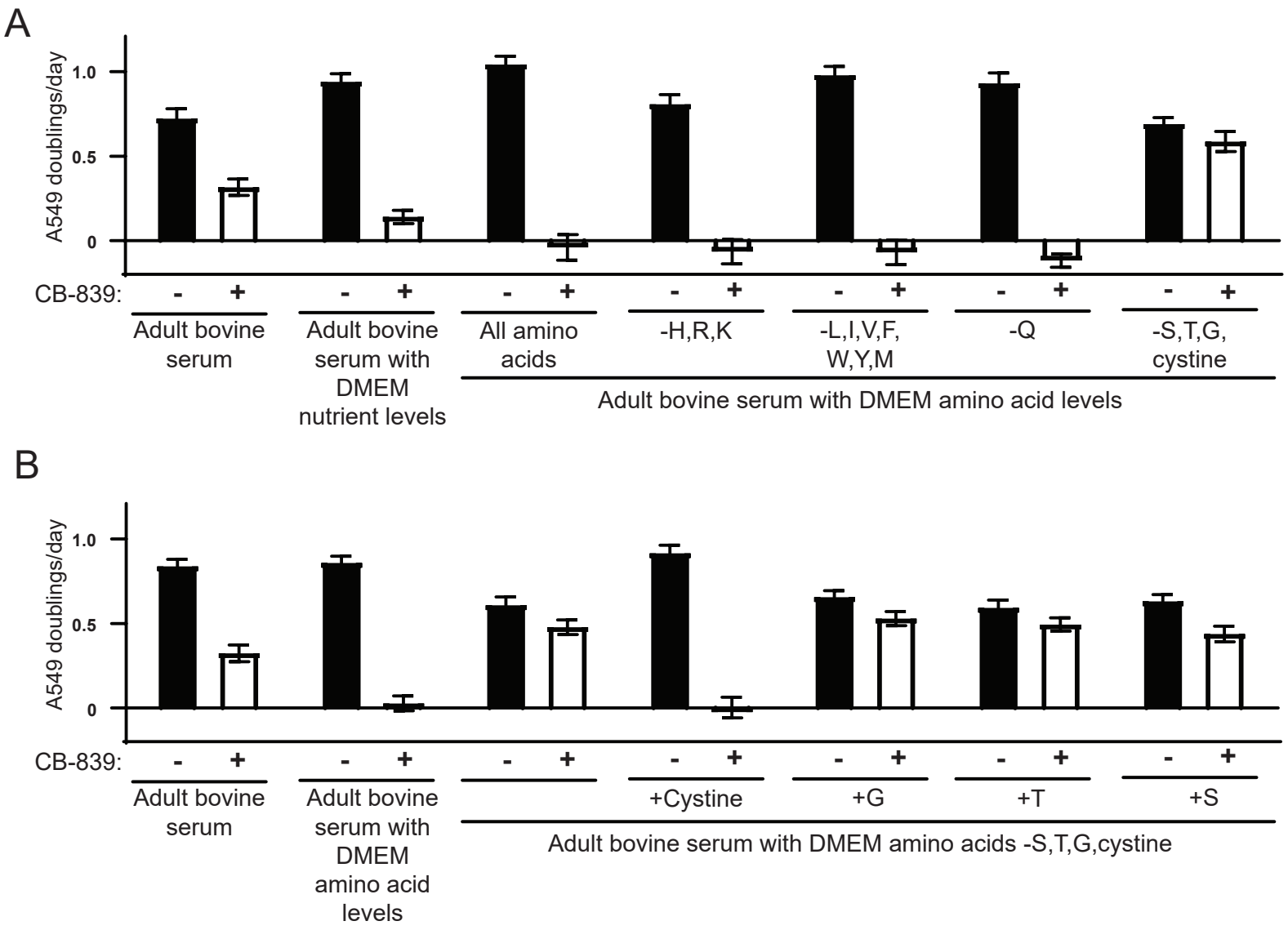

Figure 4

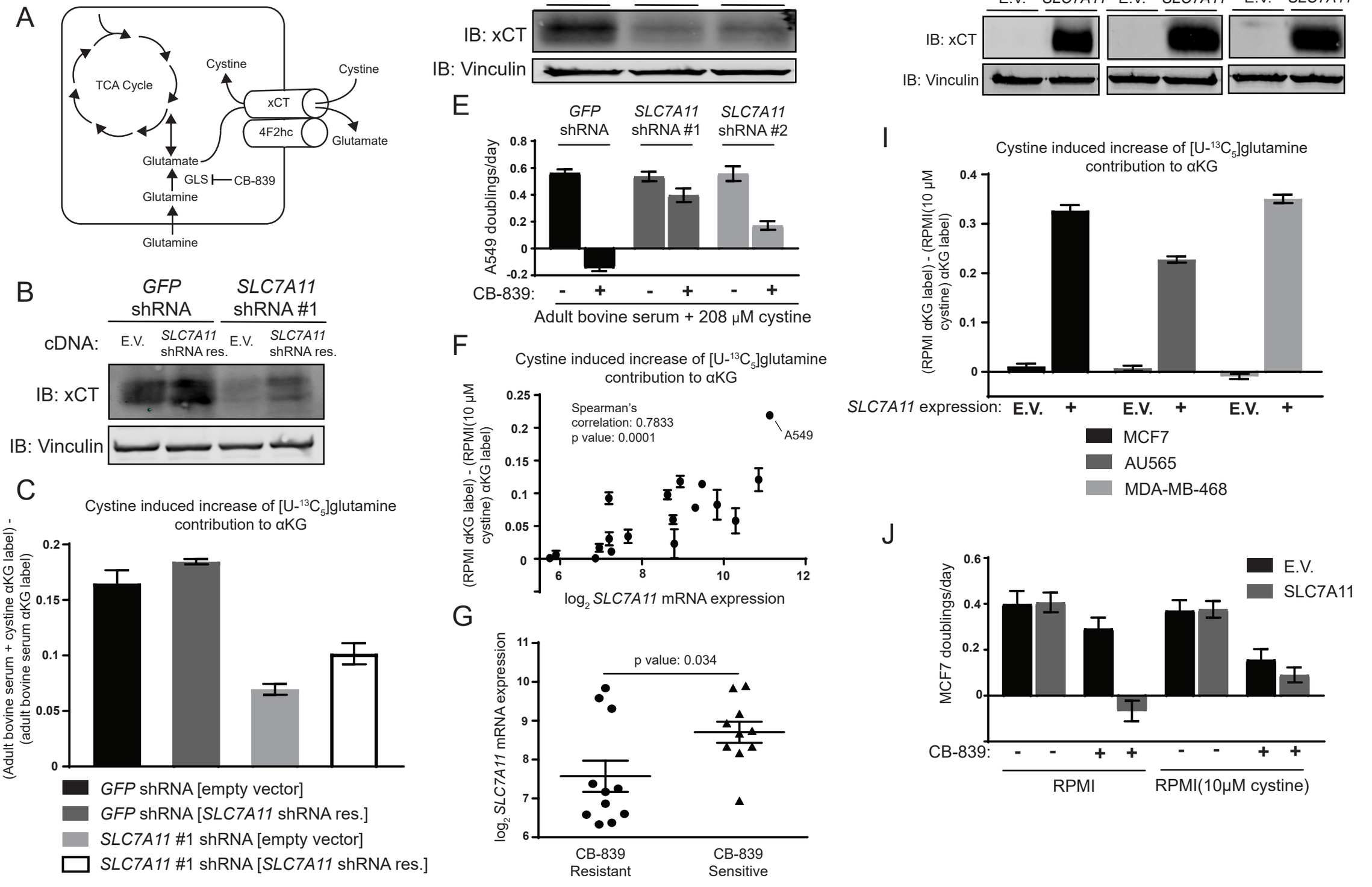
A
TCA Cycle
Cystine
Cystine
xCT
4F2hc
Glutamate
Glutamate
GLS
CB-839
Glutamine
Glutamine
B
GFP shRNA
SLC7A11 shRNA #1
cDNA:
E.V.
SLC7A11 shRNA res.
E.V.
SLC7A11 shRNA res.
IB: xCT
IB: Vinculin
C
Cystine induced increase of [U-13C5]glutamine contribution to αKG
(Adult bovine serum + cystine αKG label) - (adult bovine serum αKG label)
0.2
0.15
0.1
0.05
0
GFP shRNA [empty vector]
GFP shRNA [SLC7A11 shRNA res.]
SLC7A11 #1 shRNA [empty vector]
SLC7A11 #1 shRNA [SLC7A11 shRNA res.]
D
GFP shRNA
SLC7A11 shRNA #1
SLC7A11 shRNA #2
IB: xCT
IB: Vinculin
E
GFP shRNA
SLC7A11 shRNA #1
SLC7A11 shRNA #2
A549 doublings/day
0.8
0.6
0.4
0.2
0
-0.2
CB-839: - + - + - +
Adult bovine serum + 208 μM cystine
F
Cystine induced increase of [U-13C5]glutamine contribution to αKG
(RPMI αKG label) - (RPMI(10 μM cystine) αKG label)
Spearman's correlation: 0.7833
p value: 0.0001
A549
0.25
0.2
0.15
0.1
0.05
0
6
8
10
12
log2 SLC7A11 mRNA expression
G
log2 SLC7A11 mRNA expression
p value: 0.034
11
10
9
8
7
6
CB-839 Resistant
CB-839 Sensitive
H
MCF7
MDA-MB-468
AU565
E.V.
SLC7A11
E.V.
SLC7A11
E.V.
SLC7A11
IB: xCT
IB: Vinculin
I
Cystine induced increase of [U-13C5]glutamine contribution to αKG
(RPMI αKG label) - (RPMI(10 μM cystine) αKG label)
0.4
0.3
0.2
0.1
0
SLC7A11 expression: E.V. + E.V. + E.V. +
MCF7
AU565
MDA-MB-468
J
MCF7 doublings/day
0.6
0.4
0.2
0
E.V.
SLC7A11
CB-839: - - + + - - + +
RPMI
RPMI(10μM cystine)

Figure 4 Supplement 1

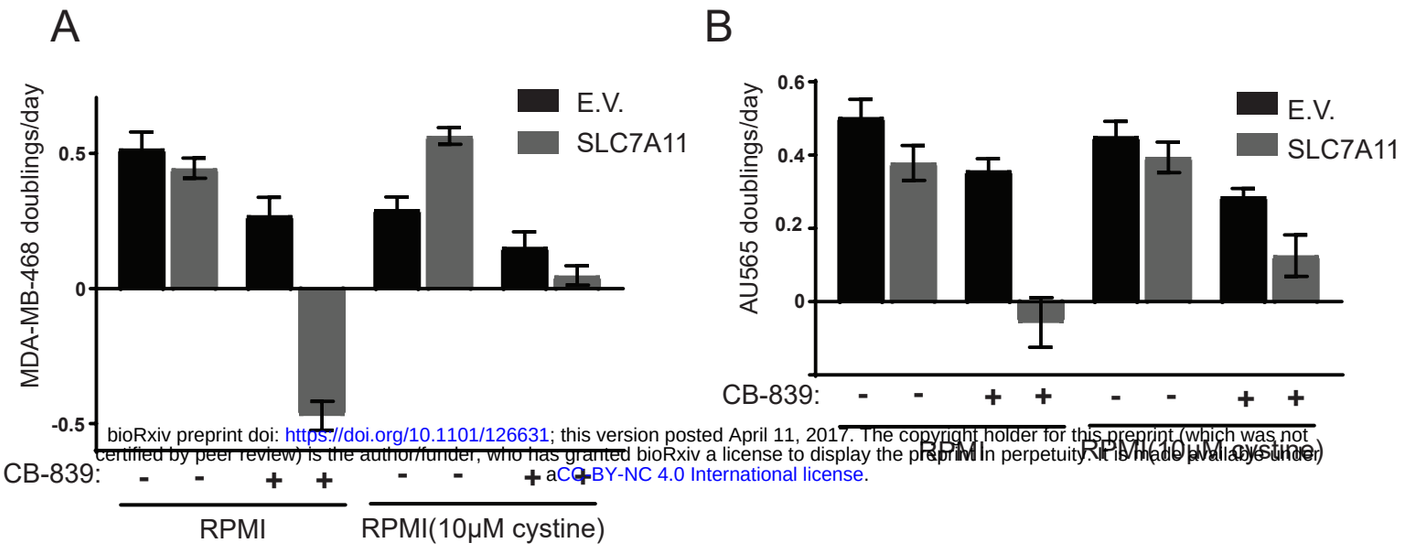

Figure 5

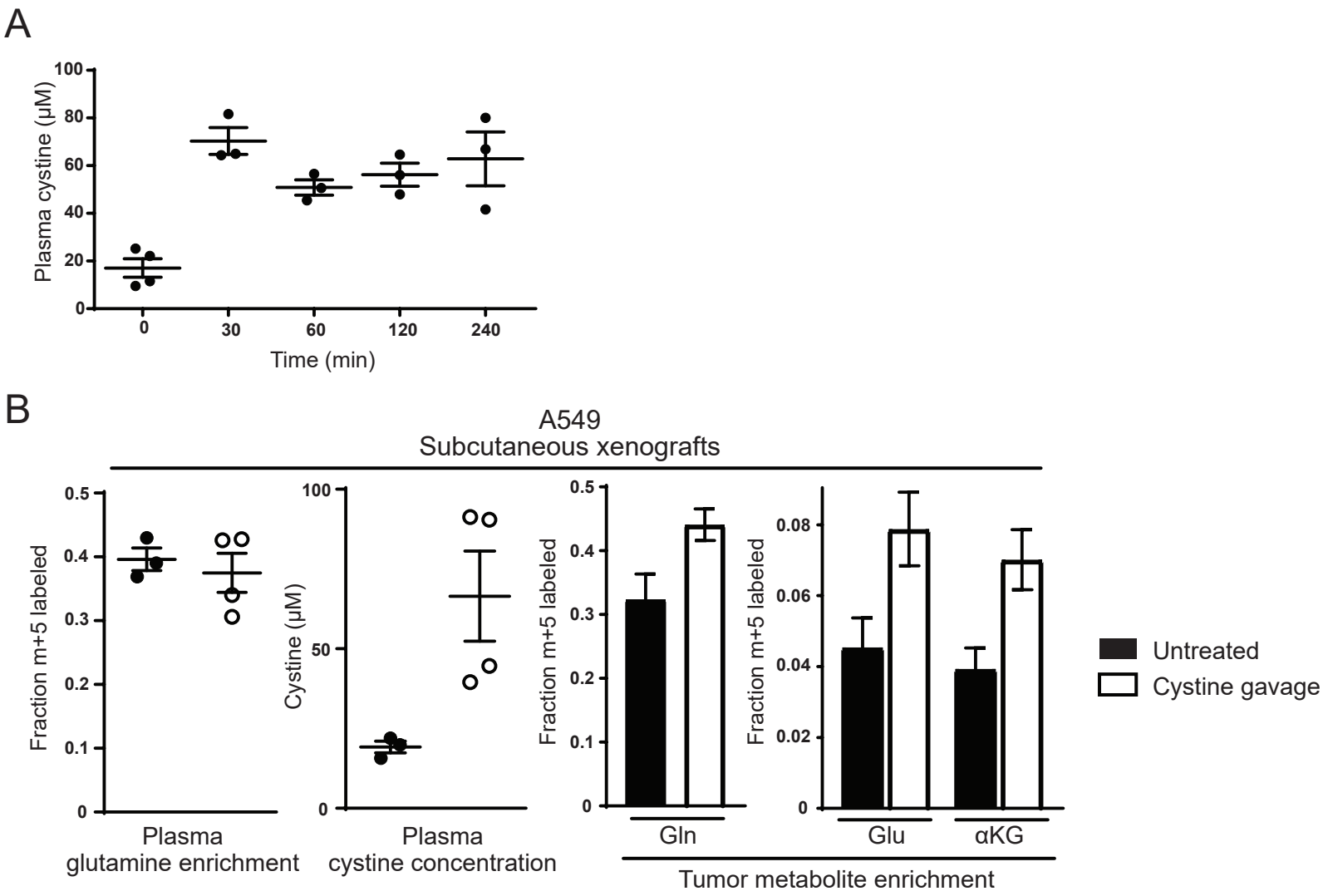

Table 1. Amino acid, glucose, pyruvate and lactate concentrations in all media used in this study compared to human plasma clinical reference values

Metabolite	Human male plasma reference range[a] [μM]	RPMI-1640 with 10% dialyzed fetal bovine serum [μM]	DMEM with 10% dialyzed fetal bovine serum [μM]	Adult bovine serum[b] [μM]	Adult bovine heparinized plasma[b] [μM]	Adult human serum[b] [μM]
Alanine	146-494	0	0	314 +/- 6	321 +/- 3	670 +/- 13
Arginine	28-96	1034	360	312 +/- 10	150 +/- 9	216 +/- 8
Aspargine	32-92	341	0	17 +/- 1	19 +/- 1	81 +/- 2
Aspartate	2-9	135	0	7.4 +/- 0.4	5.3 +/- 0.4	59.2 +/- 1.3
Cystine	24-54	187	180	0.3 +/- 0.1	2 +/- 0.1	3.4 +/- 0.2
Glutamate	6-62	122	0	192 +/- 3	120 +/-1	348 +/- 5
Glutamine	466-798	1849	3600	183 +/- 4	291 +/- 1	409 +/- 7
Glycine	147-299	120	360	302 +/- 6	221 +/- 1	409 +/- 8
Histidine	72-108	87	180	8.9 +/- 0.2	8.2 +/- 0.2	17.7 +/- 0.3
Isoleucine	46-90	344	720	112 +/- 2	84 +/- 1	114 +/- 1
Leucine	113-205	344	720	218 +/- 3	172 +/- 1	231 +/- 5
Lysine	135-243	197	720	92 +/- 2	146 +/- 1	206 +/- 4
Methionine	13-37	91	180	21 +/- 1	26 +/- 1	39 +/- 1
Phenylalanine	46-74	82	360	92 +/- 2	68 +/- 1	144 +/- 3
Proline	97-297	157	0	88 +/- 2	61 +/- 1	301 +/- 4
Serine	89-165	257	360	119 +/- 2	74 +/- 1	237 +/- 5
Threonine	92-180	151	720	63 +/- 1	50 +/- 1	192 +/- 3
Tryptophan	25-65	22	72	ND	ND	ND
Tyrosine	37-77	99	360	56 +/- 1	47 +/- 1	101 +/- 3
Valine	179-335	154	720	251 +/- 5	181 +/- 2	325 +/- 6
Glucose		9990	22500	3932 +/- 26	8403 +/- 33	2407 +/- 23
Pyruvate	27-160	0	900	9.4 +/- 0.2	70.8 +/- 0.5	10.3 +/- 0.7
Lactate		0	0	10878 +/- 217	9291 +/- 61	9250 +/- 178

[a] Shown is the range +/- 2 standard deviations from the mean value for the indicated metabolite. These values are from (Blau, 2003). [b] Shown are the mean values +/- the standard error of the mean for the indicated metabolites as determined by GC-MS (see **Materials and Methods** for detailed procedure), except glucose concentration, which was determined using a YSI bioanalyzer. All samples were analyzed in triplicate. ND indicates that the metabolite was not detected.